Synthesis, stability, and (de)hydrogenation catalysis by normal and abnormal alkene- and picolyl-tethered NHC ruthenium complexes

Frederick P. Malan,[†] Eric Singleton,[†] Petrus H. van Rooyen,[†] Marilé Landman[†*] and Martin Albrecht[‡*]

[†] *Department of Chemistry, University of Pretoria, 02 Lynnwood Road, Hatfield, Pretoria, 0002, South Africa.*

[‡] *Department of Chemistry and Biochemistry, Universität Bern, Freiestrasse 3, 3012 Bern, Switzerland.*

Supporting Information

1. Synthesis, characterization, and NMR spectra of [HL1]Cl–[HL4]Cl

General synthesis of imidazolium salts: To an acetonitrile (20 mL) solution of 1,2-dimethylimidazole (42 mmol, **L1**, **L2**) /2,3,5-trimethylimidazole (42 mmol, **L3**)/1-(2-methylpropenyl)-2-isopropylimidazole (50 mmol, **L4**) was added the respective alkyl halide (1-chloro-2-methylpropene (**L1**, **L3**, **L4**) or picolyl chloride (**L2**)) (1 equivalent), and the resulting mixture heated under reflux overnight. After cooling, the reaction mixture was concentrated *in vacuo*, and washed with a 1:1 v/v Et_2O/Et_2OAc mixture (3 × 15 mL). The resulting oil/solid was concentrated in vacuo to give the respective salts [H**L1**]Cl–[H**L4**]Cl.

[H**L1**]Cl: Yield: 93%. ^{1}H NMR ($CDCl_3$): δ_H = 1.61 (s, 3H, =CCH_3), 2.63 (s, 3H, C_{imi}-Me), 3.91 (s, 3H, NCH_3), 4.57 (s, 1H, =CH_2), 4.76 (s, 2H, NCH_2), 4.88 (s, 1H, =CH_2), 7.51 (d, $^{3}J_{HH}$ = 2 Hz, 1H, C_{imi}H), 7.78 (d, $^{3}J_{HH}$ = 2 Hz, 1H, C_{imi}H). ^{13}C{^{1}H} NMR ($CDCl_3$): δ_C = 10.2 (s, =C*C*H_3), 19.7 (s, C_{imi}-*C*H_3), 35.7 (s, NCH_3), 54.0 (s, NCH_2), 114.7 (s, =C*C*H_2), 121.8 (s, C_{imi}H), 122.9 (s, C_{imi}H), 137.6 (s, =*C*CH_2), 144.0 (s, NCN).

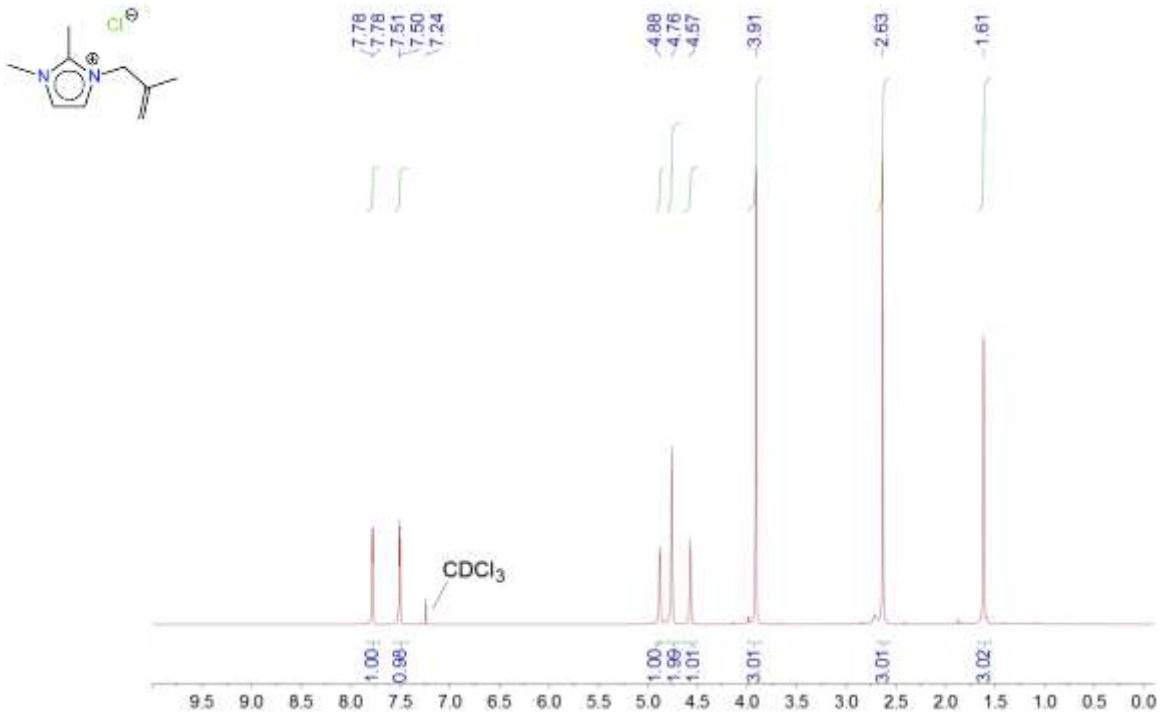

Figure S1. ^{1}H NMR spectrum (400 MHz, 298 K, $CDCl_3$) of [H**L1**]Cl.

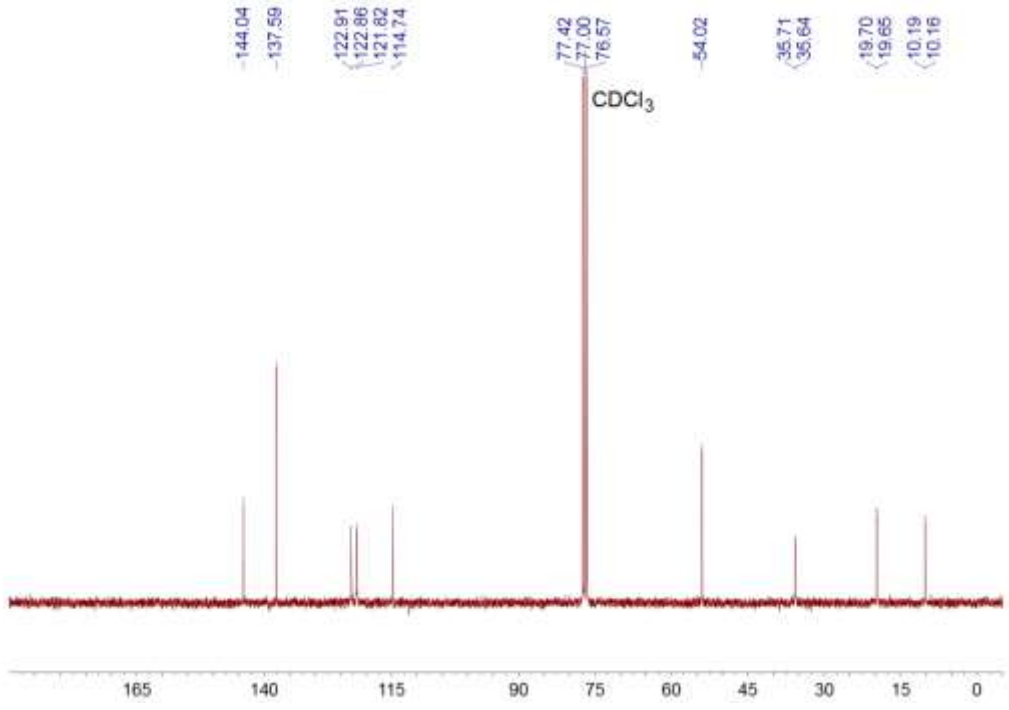

Figure S2. ^{13}C NMR spectrum (100 MHz, 298 K, $CDCl_3$) of [H**L1**]Cl.

[H**L2**]Cl: Yield: 88%. ^{1}H NMR (CD_3CN): δ_H = 2.60 (s, 3H, C_{imi}-Me), 3.80 (s, 3H, NCH_3), 5.57 (s, 2H, NCH_2), 7.33 (dd, $^{3}J_{HH}$ = 3 and 6 Hz, 1H, H_{py}), 7.46 (d, $^{3}J_{HH}$ = 2 Hz, 1H, $C_{imi}H$), 7.52 (d, $^{3}J_{HH}$ = 8 Hz, 1H, H_{py}), 7.64 (d, $^{3}J_{HH}$ = 2 Hz, 1H, $C_{imi}H$), 7.84 (ddd, $^{3}J_{HH}$ = 2 and 8 Hz, 1H, H_{py}), 8.52 (d, $^{3}J_{HH}$ = 4 Hz, 1H, $C_{imi}H$). $^{13}C\{^{1}H\}$ NMR (CD_3CN): δ_C = 9.7 (s, C_{imi}-CH_3), 35.0 (s, NCH_3), 52.0 (s, NCH_2), 121.9 (s, $C_{imi}H$), 122.4 (s, $C_{imi}H$), 122.6 (s, C_{py}), 123.6 (s, C_{py}), 137.4 (s, C_{py}), 145.5 (s, C_{py}), 149.7 (s, C_{py}), 153.4 (s, NCN).

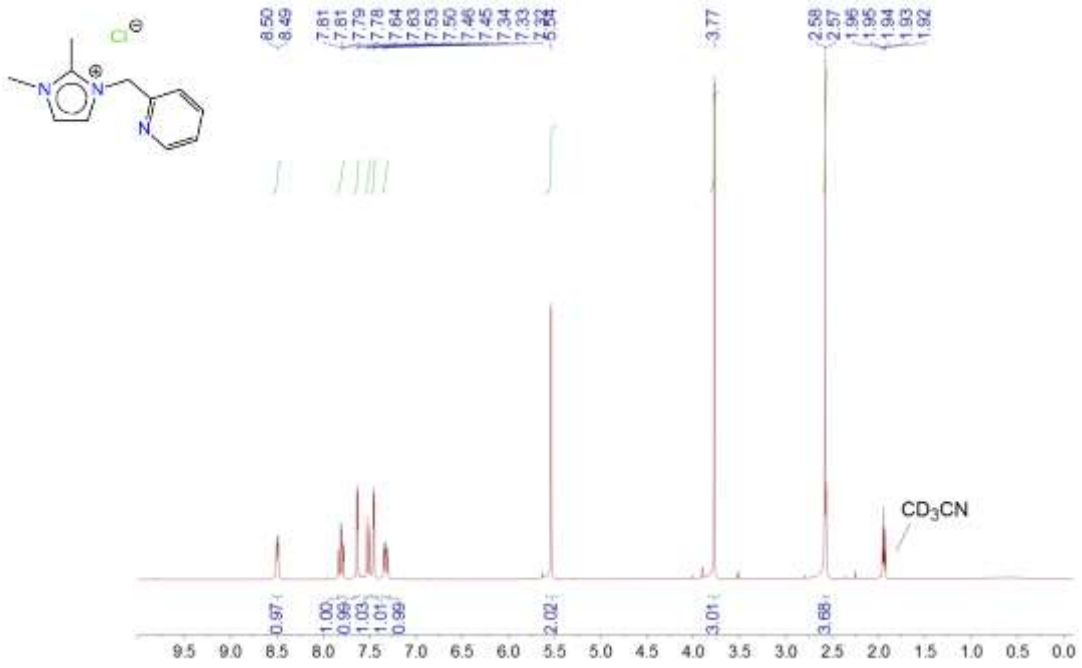

Figure S3. ^{1}H NMR spectrum (400 MHz, 298 K, CD_3CN) of [H**L2**]Cl.

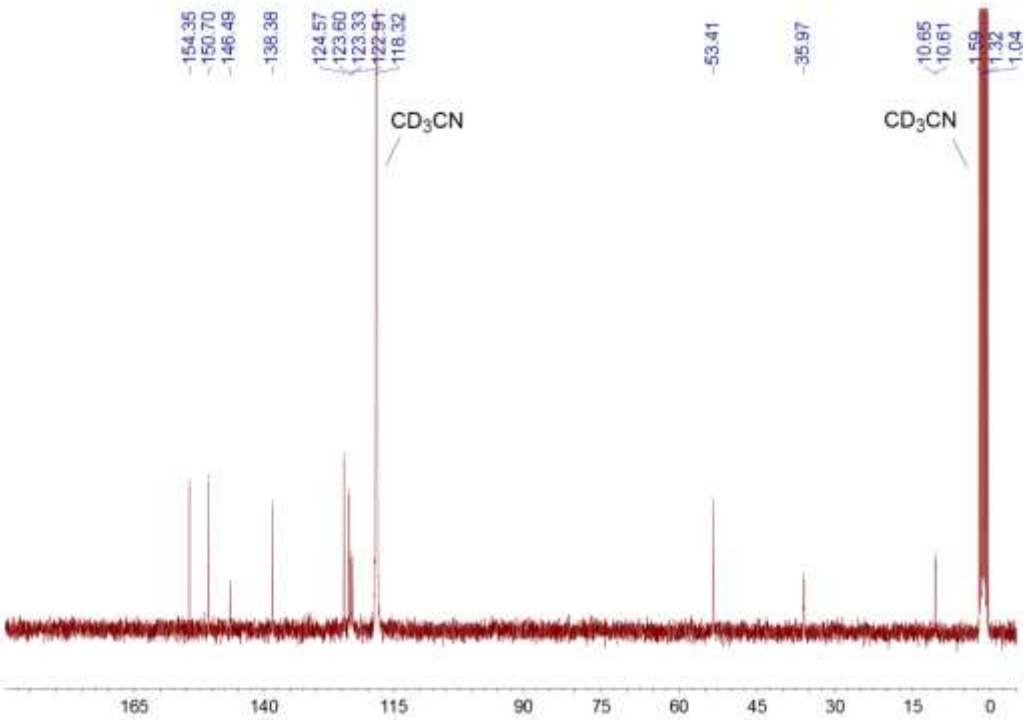

Figure S4. ^{13}C NMR spectrum (100 MHz, 298 K, CD_3CN) of [H**L2**]Cl.

[H**L3**]Cl: Yield: 53%. ^{1}H NMR ($CDCl_3$): δ_H = 1.53 (s, 3H, =CCH_3), 2.12 (s, 3H, C_{imi}-Me), 2.55 (s, 3H, C_{imi}-Me), 3.64 (s, 3H, NCH_3), 4.51 (s, 1H, =CH_2), 4.60 (s, 2H, NCH_2), 4.79 (s, 1H, =CH_2), 7.14 (s, 1H, C_{imi}H). ^{13}C{^{1}H} NMR ($CDCl_3$): δ_C = 10.4 (s, =C*C*H_3), 13.7 (s, C_{imi}-*C*H_3), 19.5 (s, C_{imi}-*C*H_3), 32.3 (s, NCH_3), 53.6 (s, NCH_2), 114.5 (s, =C*C*H_2), 118.7 (s, C_{imi}H), 129.7 (s, C_{imi}H), 137.4 (s, =*C*CH_2), 143.6 (s, NCN).

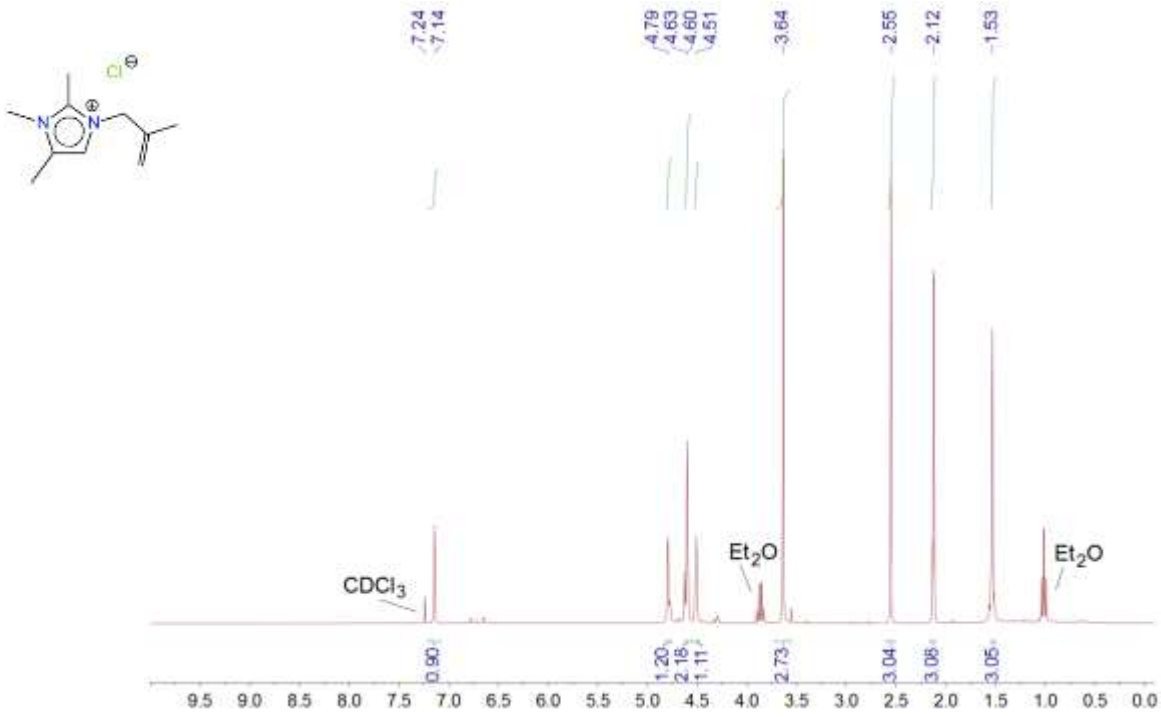

Figure S5. ^{1}H NMR spectrum (400 MHz, 298 K, $CDCl_3$) of [H**L3**]Cl.

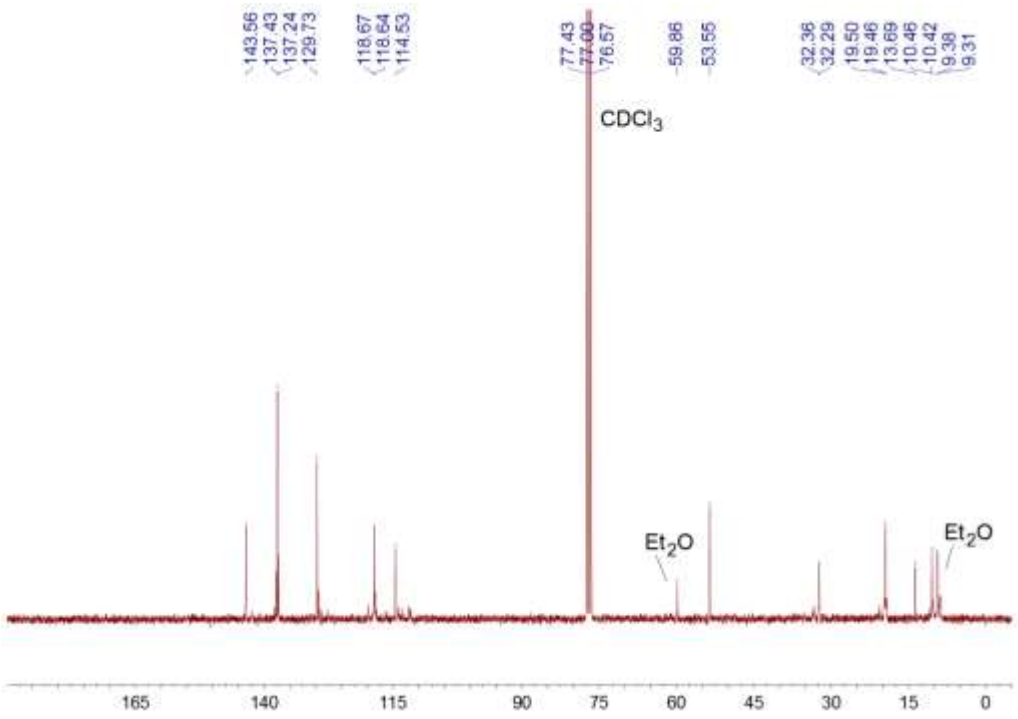

Figure S6. ^{13}C NMR spectrum (100 MHz, 298 K, $CDCl_3$) of [H**L3**]Cl.

[H**L4**]Cl: Yield: 90%. ^{1}H NMR (CD_3CN): δ_H = 1.43 (d, $^{3}J_{HH}$ = 7 Hz, 6H, $CH(CH_3)_2$), 1.78 (s, 6H, $CH(CH_3)_2$), 3.52 (m, 1H, $CH(CH_3)_2$), 4.58 (s, 2H, $=CH_2$), 4.82 (s, 4H, NCH_2), 5.06 (s, 2H, $=CH_2$), 7.47 (s, 2H, $C_{imi}H$). ^{13}C{^{1}H} NMR (CD_3CN): δ_C = 19.2 (s, $C(CH_3)_2$), 20.0 (s, $C(CH_3)_2$), 26.2 (s, $=CCH_2$), 54.6 (s, NCH_2), 114.0 (s, $=CCH_2$), 123.7 (s, $C_{imi}H$), 140.8 (s, $C(CH_3)_2$), 151.4 (s, NCN).

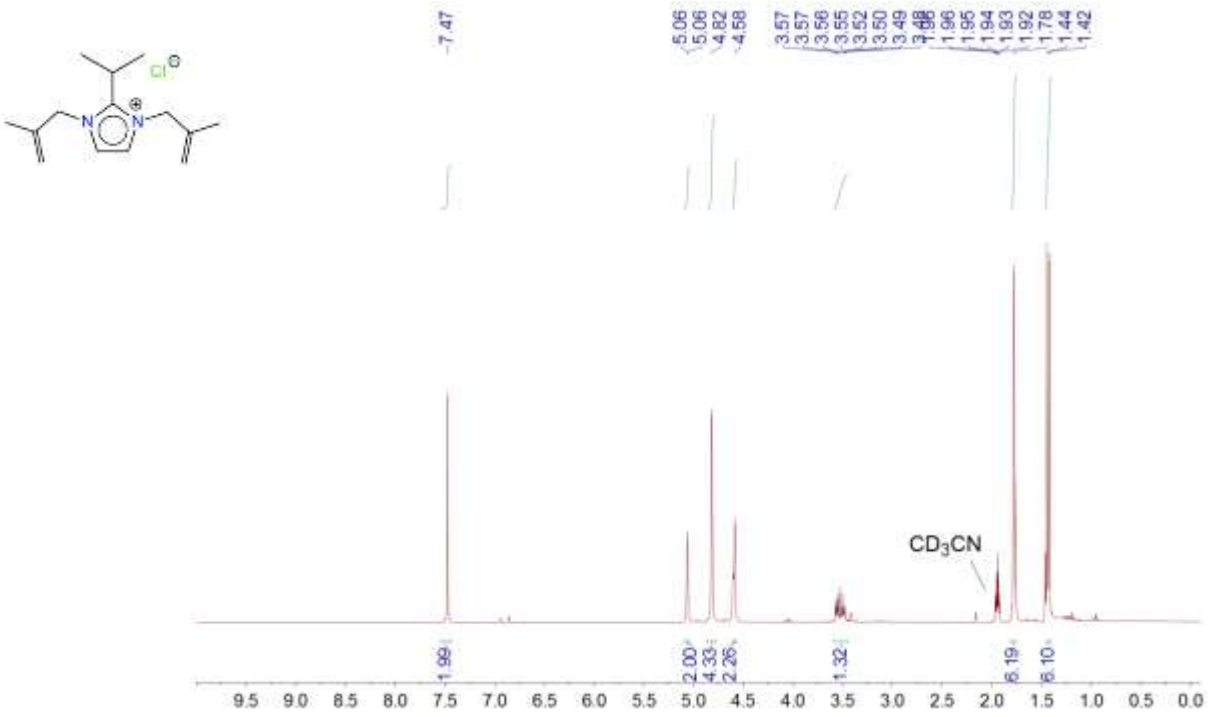

Figure S7. ^{1}H NMR spectrum (400 MHz, 298 K, CD_3CN) of [H**L4**]Cl.

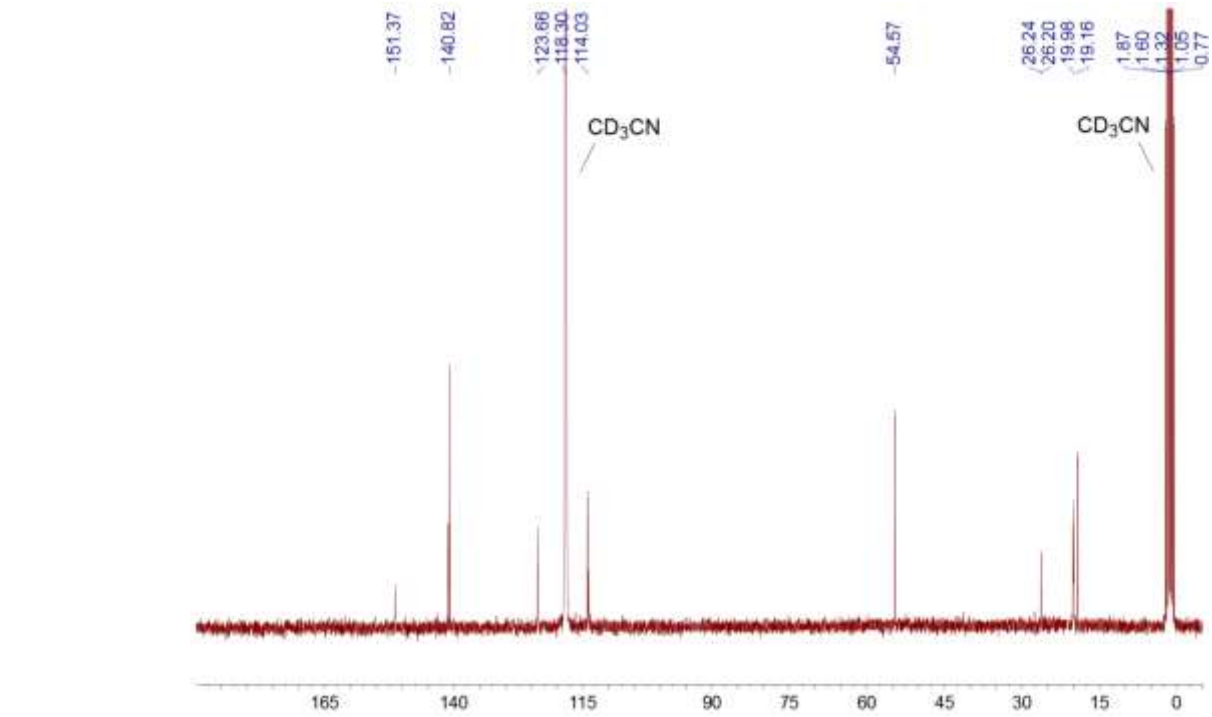

Figure S8. ^{13}C NMR spectrum (100 MHz, 298 K, CD_3CN) of [H**L4**]Cl.

2. ^{1}H, ^{13}C, and ^{31}P NMR spectra of complexes 1-10

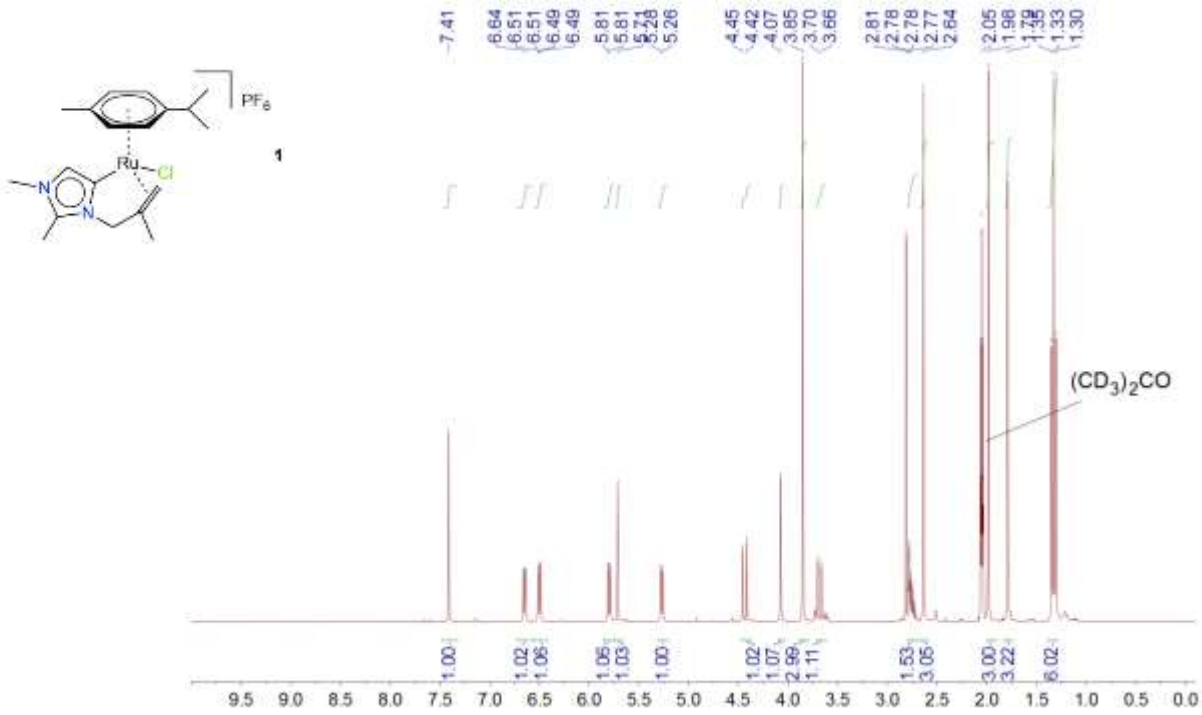

Figure S9. ^{1}H NMR spectrum (300 MHz, 298 K, $(CD_3)_2CO$) of complex **1**.

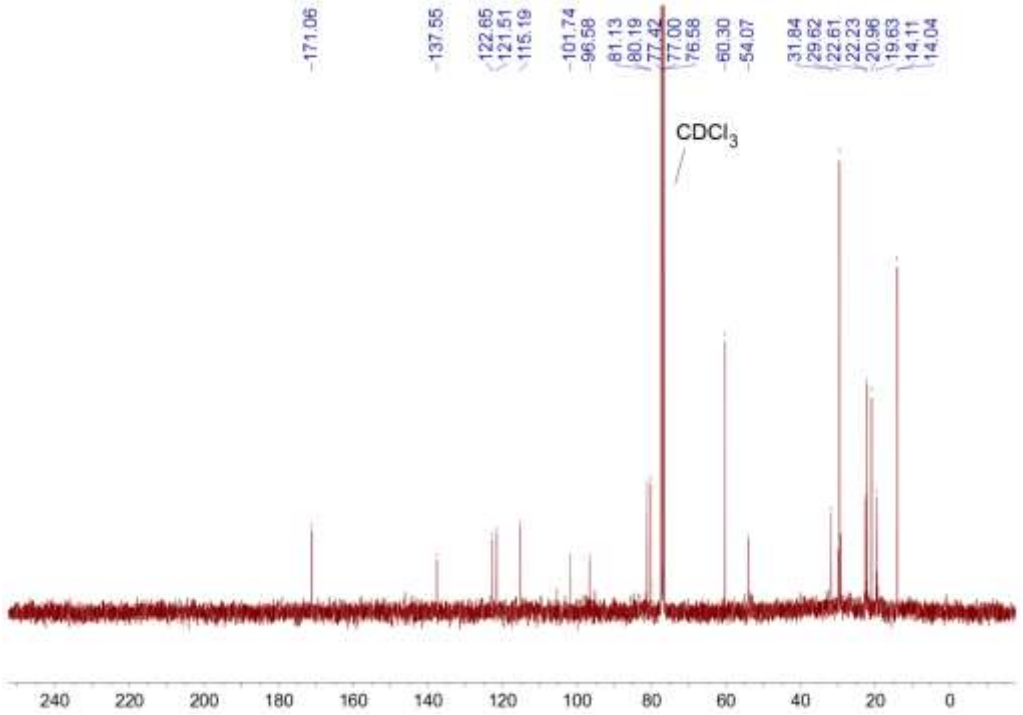

Figure S10. ^{13}C NMR spectrum (76 MHz, 298 K, $CDCl_3$) of complex **1**.

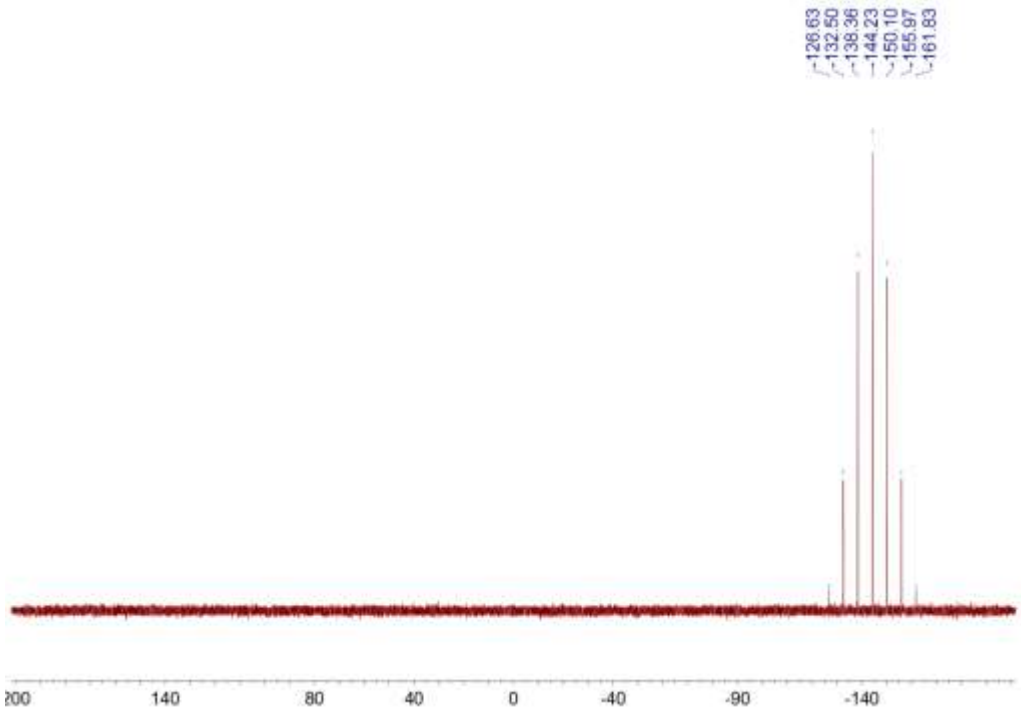

Figure S11. ^{31}P NMR spectrum (122 MHz, 298 K, $CDCl_3$) of complex **1**.

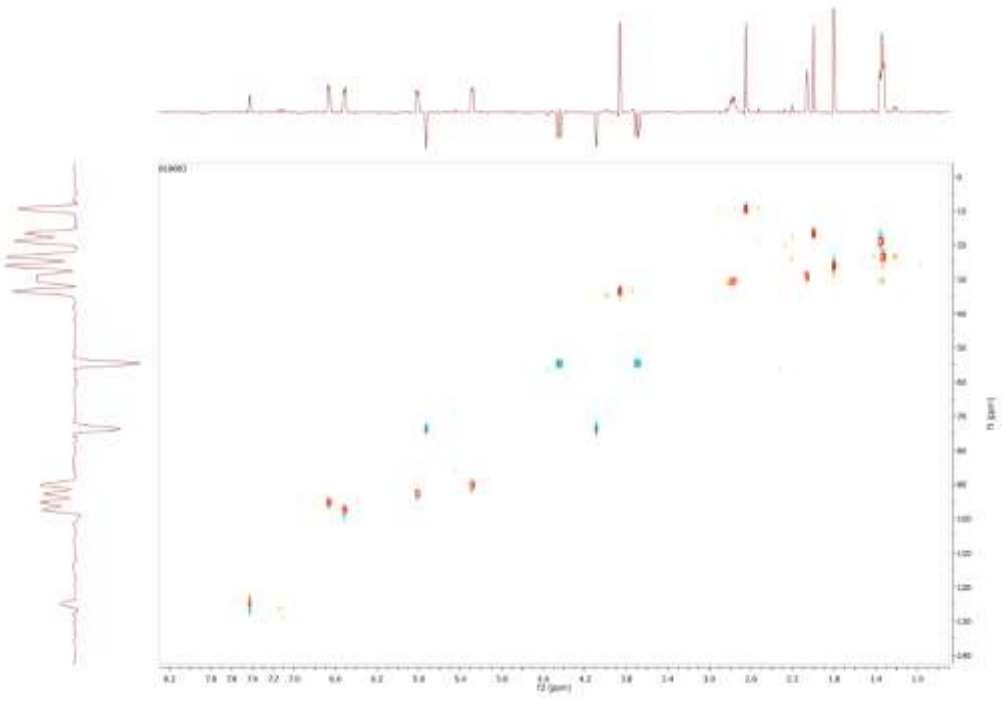

Figure S12. HSQC NMR spectrum (400, 100 MHz, 298 K, $(CD_3)_2CO$) of complex **1**.

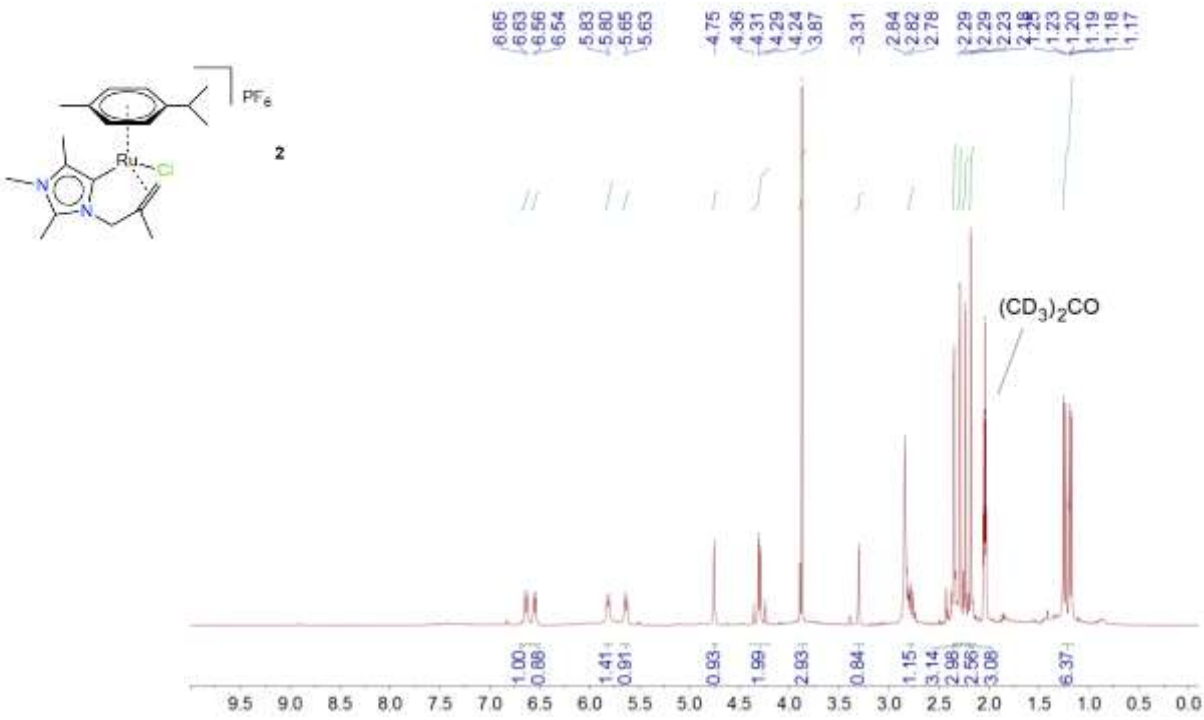

Figure S13. ^{1}H NMR spectrum (300 MHz, 298 K, $(CD_3)_2CO$) of complex **2**.

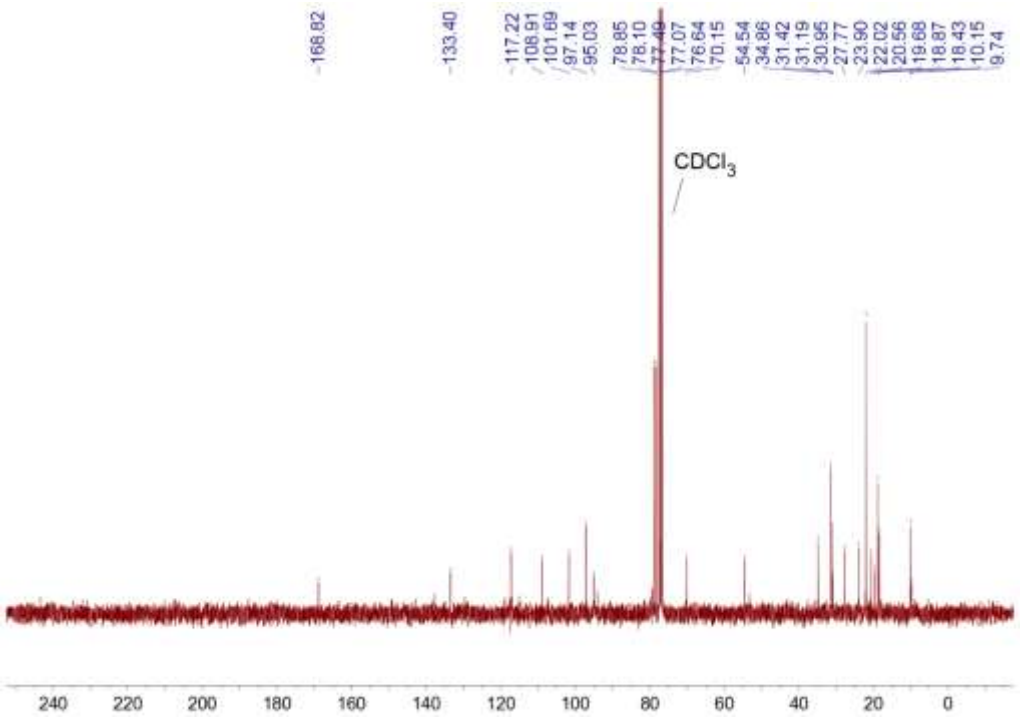

Figure S14. ^{13}C NMR spectrum (76 MHz, 298 K, $CDCl_3$) of complex **2**.

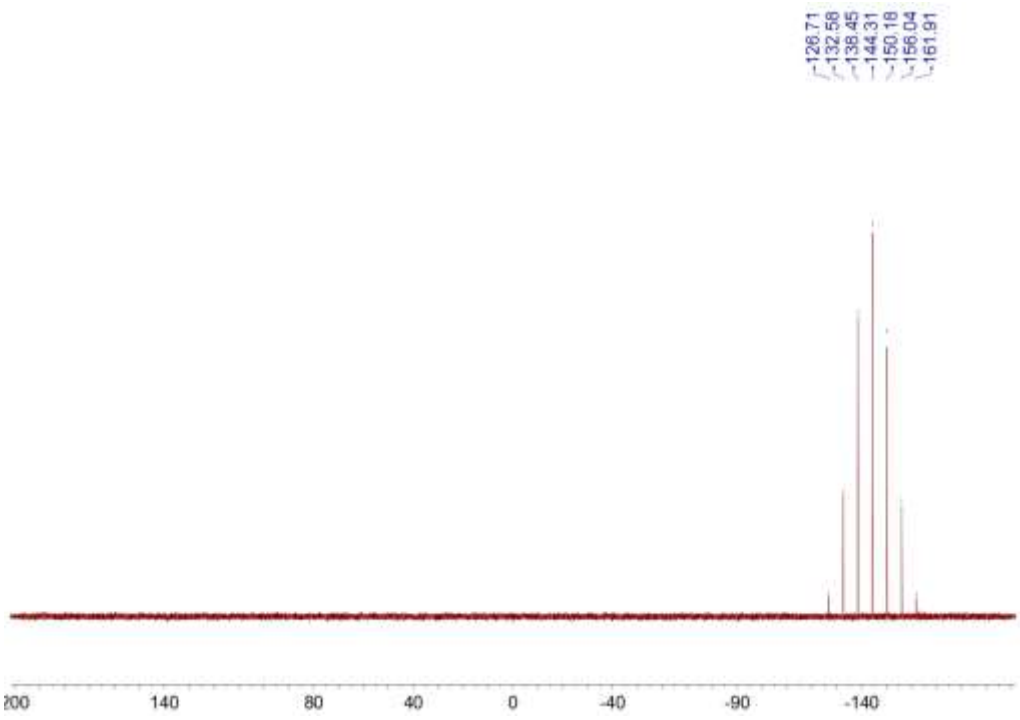

Figure S15. ^{31}P NMR spectrum (122 MHz, 298 K, $CDCl_3$) of complex **2**.

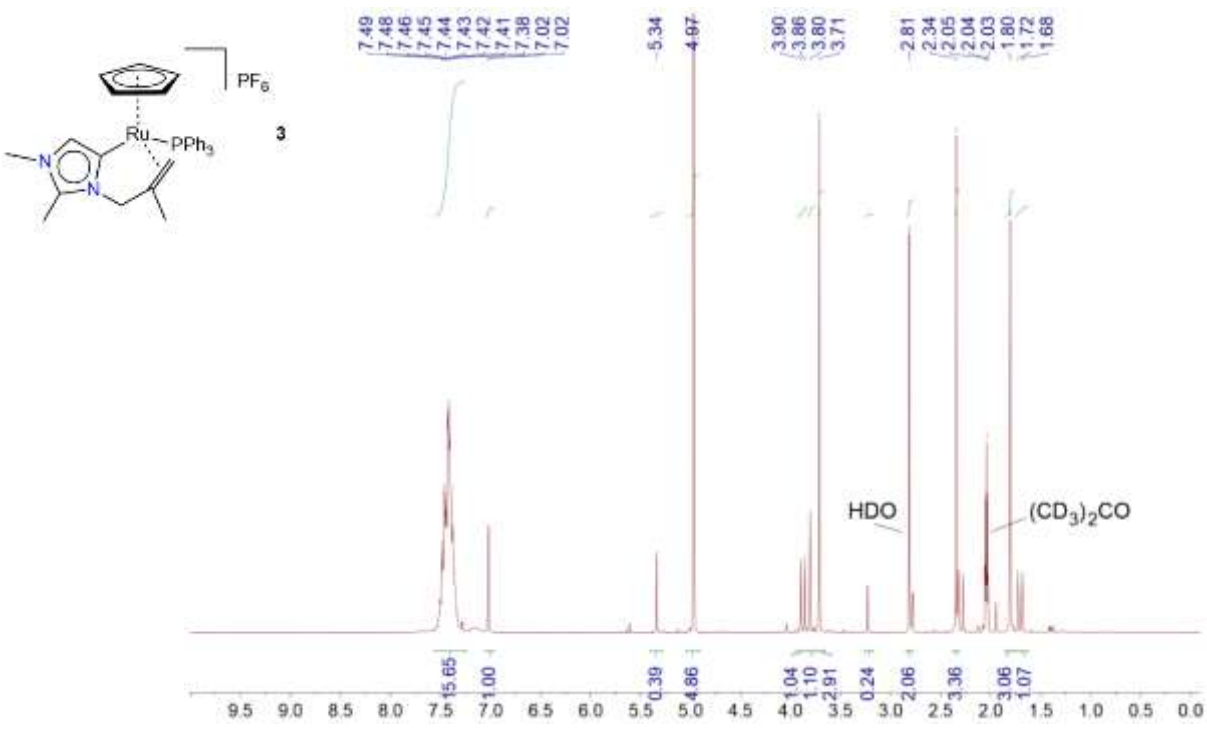

Figure S16. ^{1}H NMR spectrum (300 MHz, 298 K, $(CD_3)_2CO$) of complex **3**.

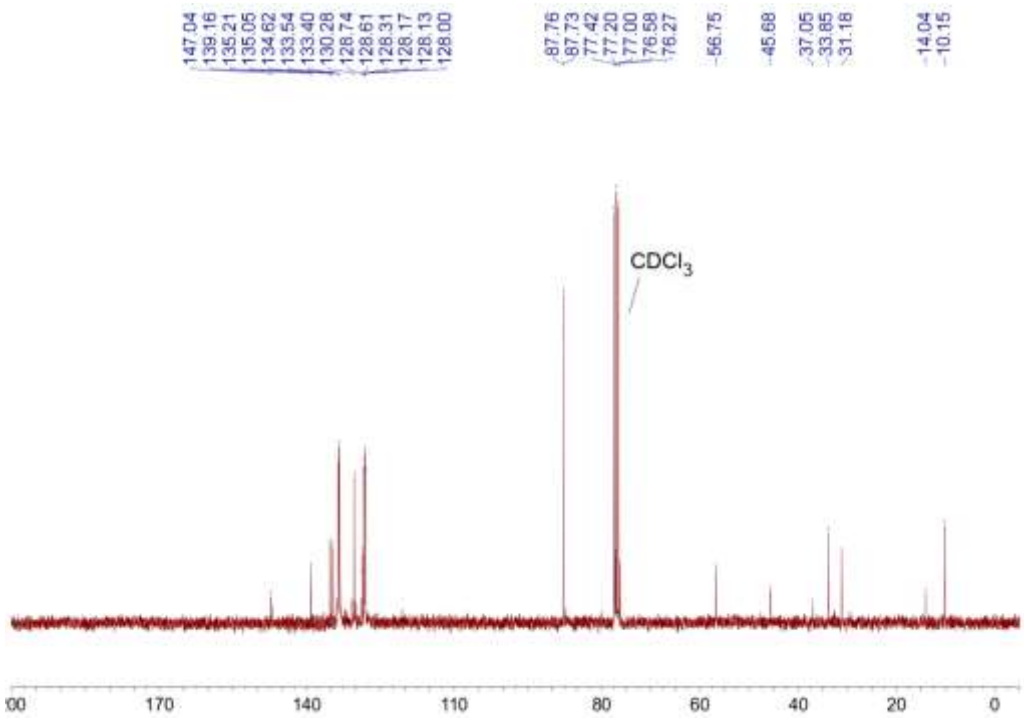

Figure S17. ^{13}C NMR spectrum (76 MHz, 298 K, $CDCl_3$) of complex **3**.

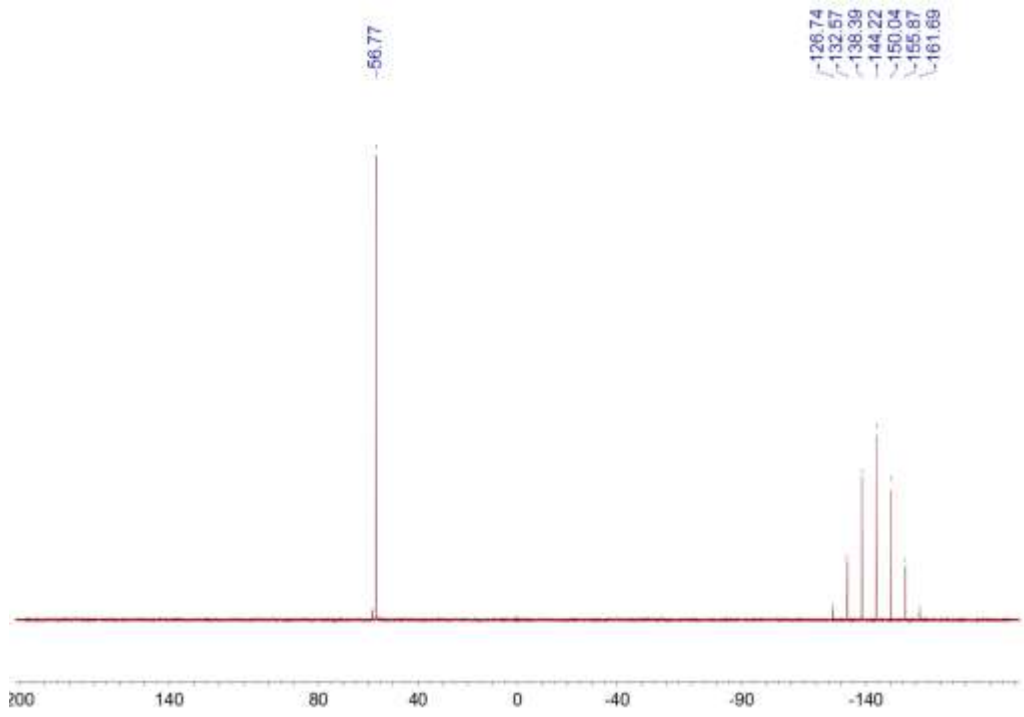

Figure S18. ^{31}P NMR spectrum (122 MHz, 298 K, $CDCl_3$) of complex **3**.

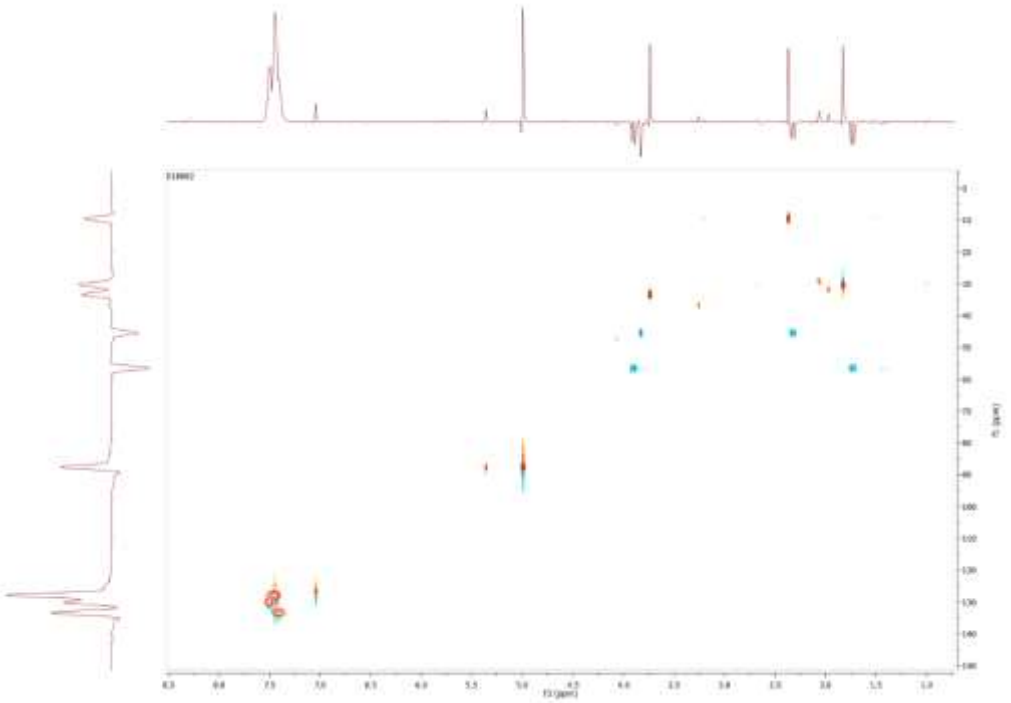

Figure S19. HSQC NMR spectrum (400, 100 MHz, 298 K, $(CD_3)_2CO$) of complex **3**.

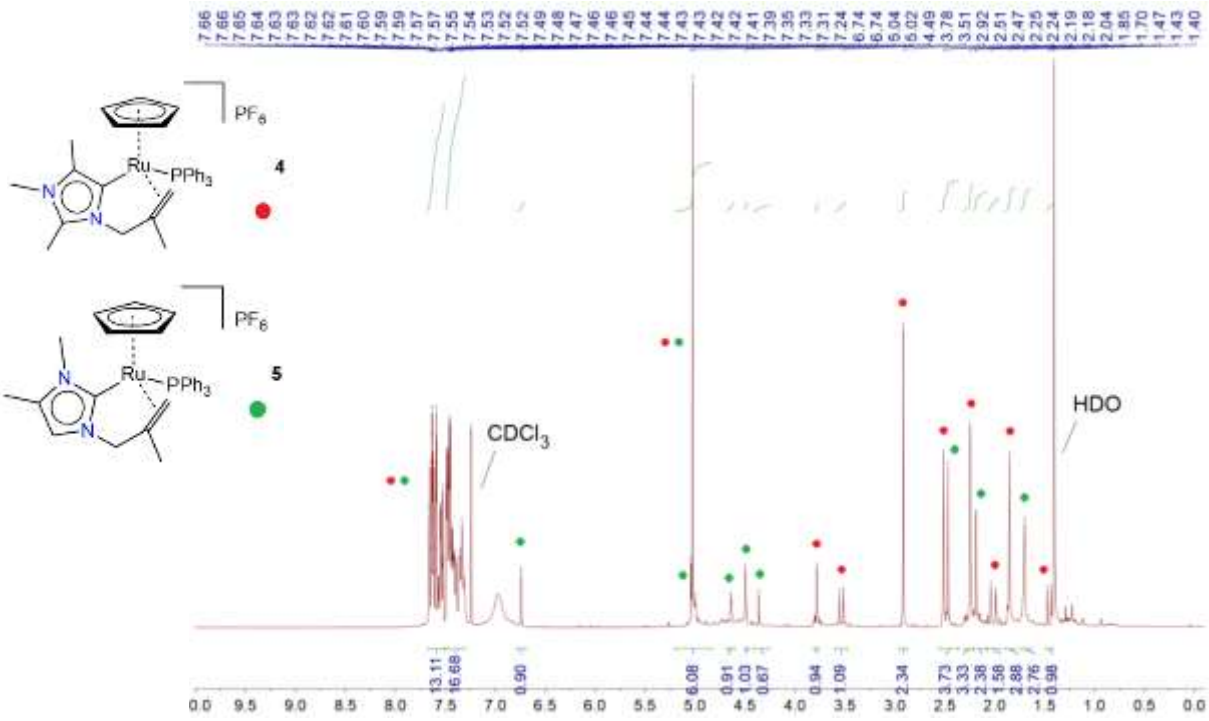

Figure S20. ^1H NMR spectrum (300 MHz, 298 K, $CDCl_3$) of complexes **4/5**.

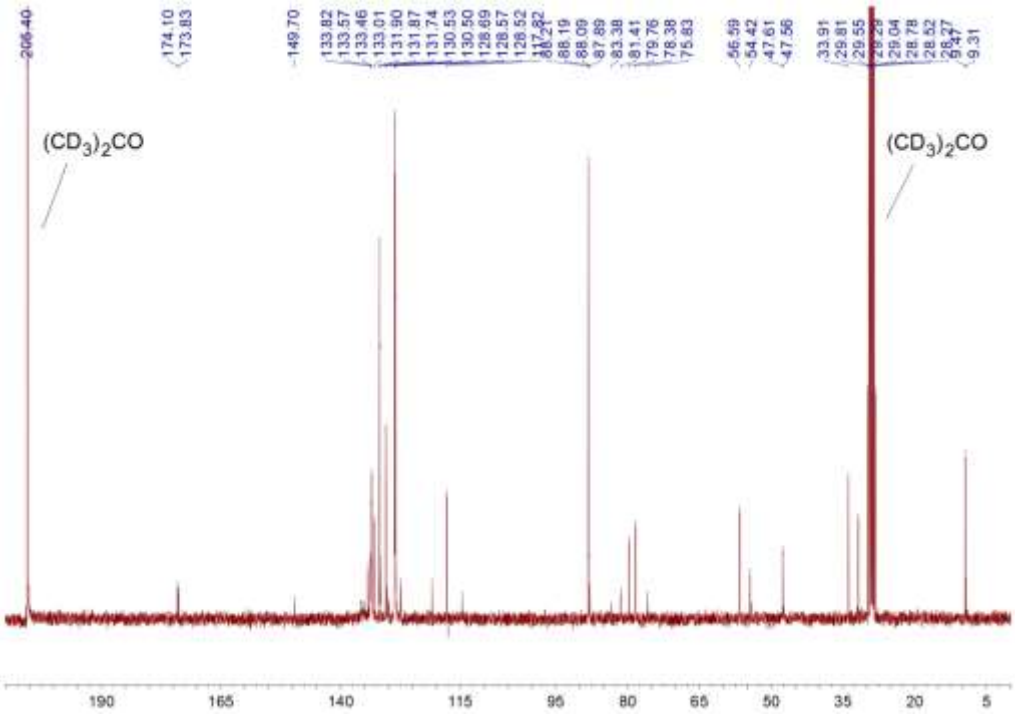

Figure S21. ^{13}C NMR spectrum (76 MHz, 298 K, $(CD_3)_2CO$) of complexes **4/5**.

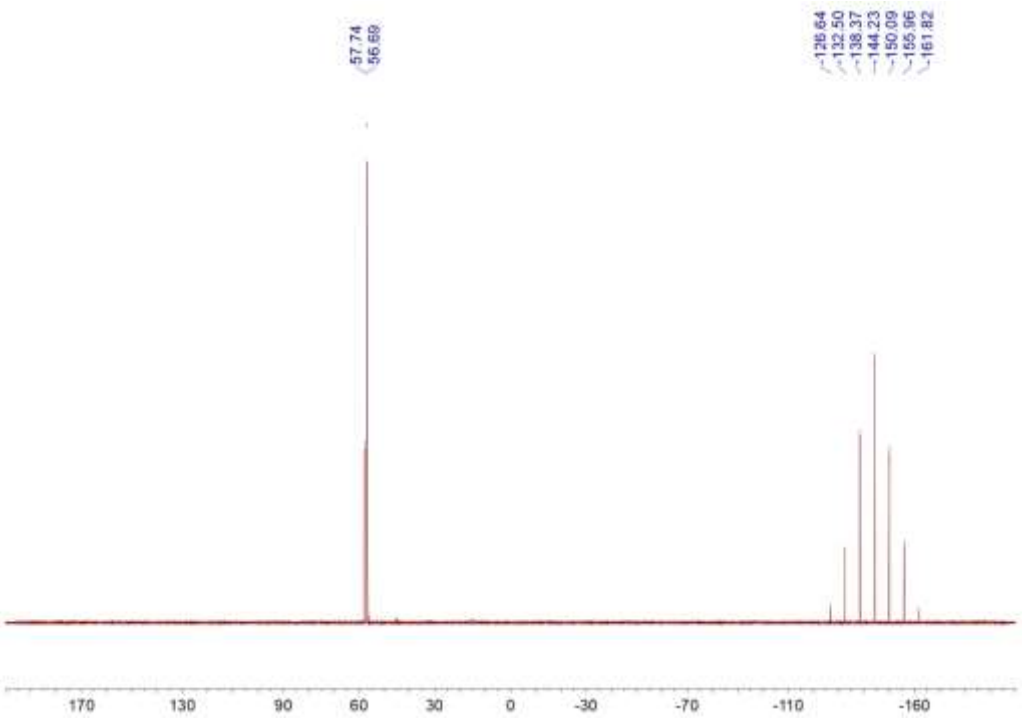

Figure S22. ^{31}P NMR spectrum (122 MHz, 298 K, $CDCl_3$) of complexes **4/5**.

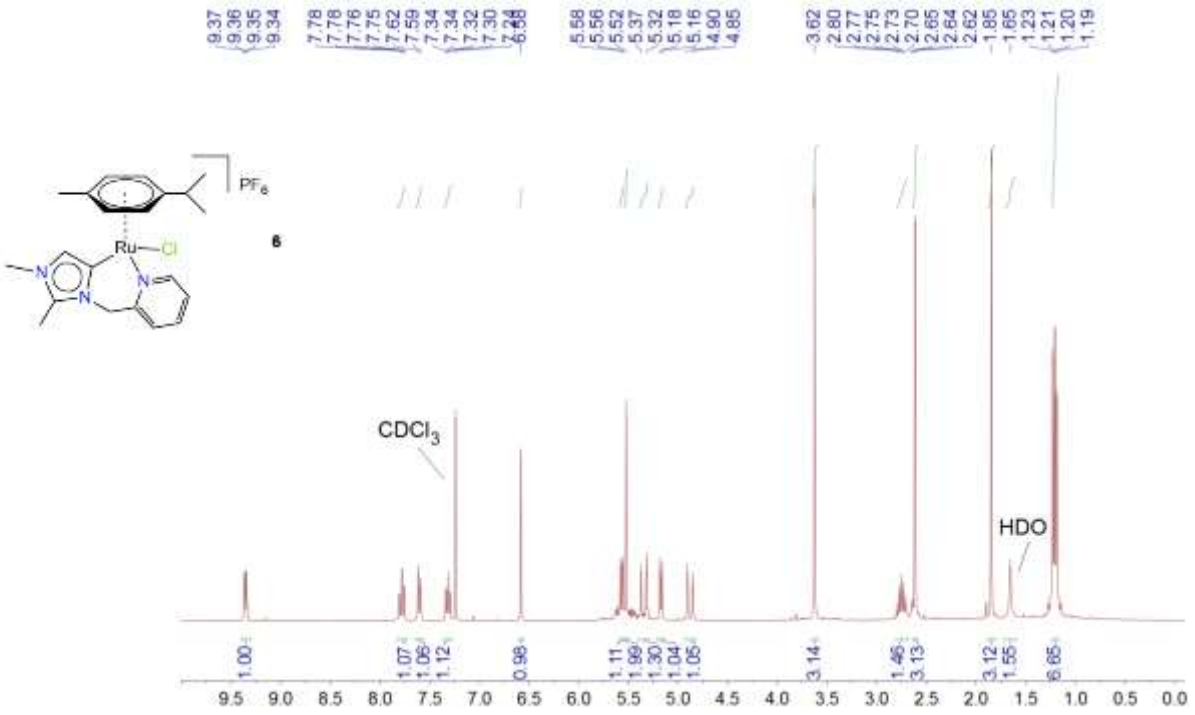

Figure S23. ^{1}H NMR spectrum (300 MHz, 298 K, $CDCl_3$) of complex **6**.

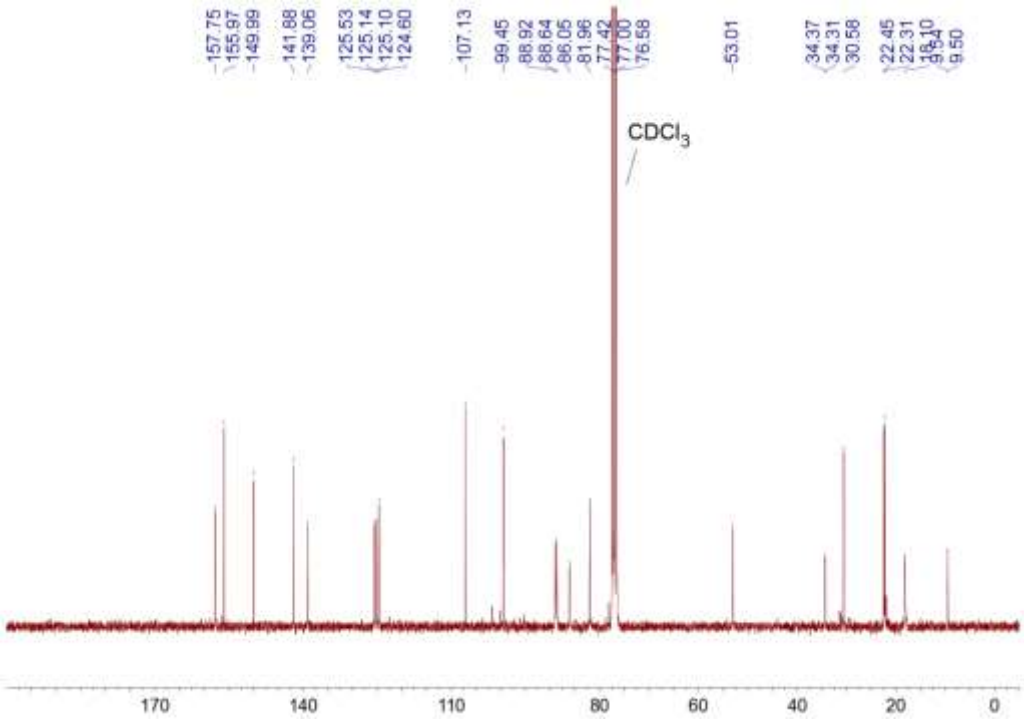

Figure S24. ^{13}C NMR spectrum (76 MHz, 298 K, $CDCl_3$) of complex **6**.

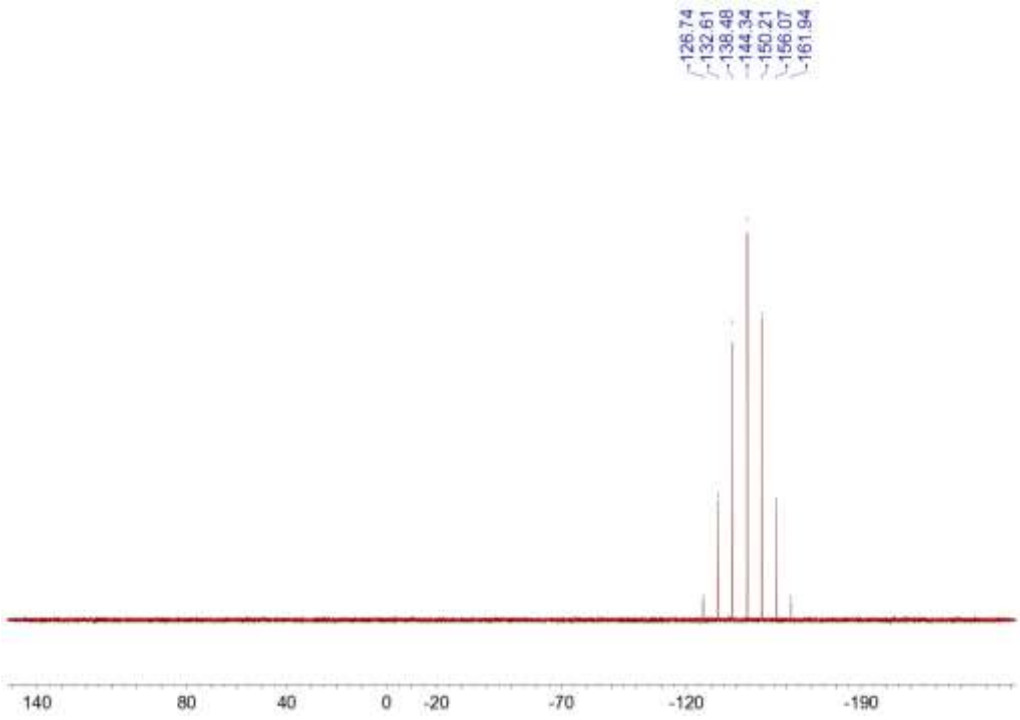

Figure S25. ^{31}P NMR spectrum (122 MHz, 298 K, $CDCl_3$) of complex **6**.

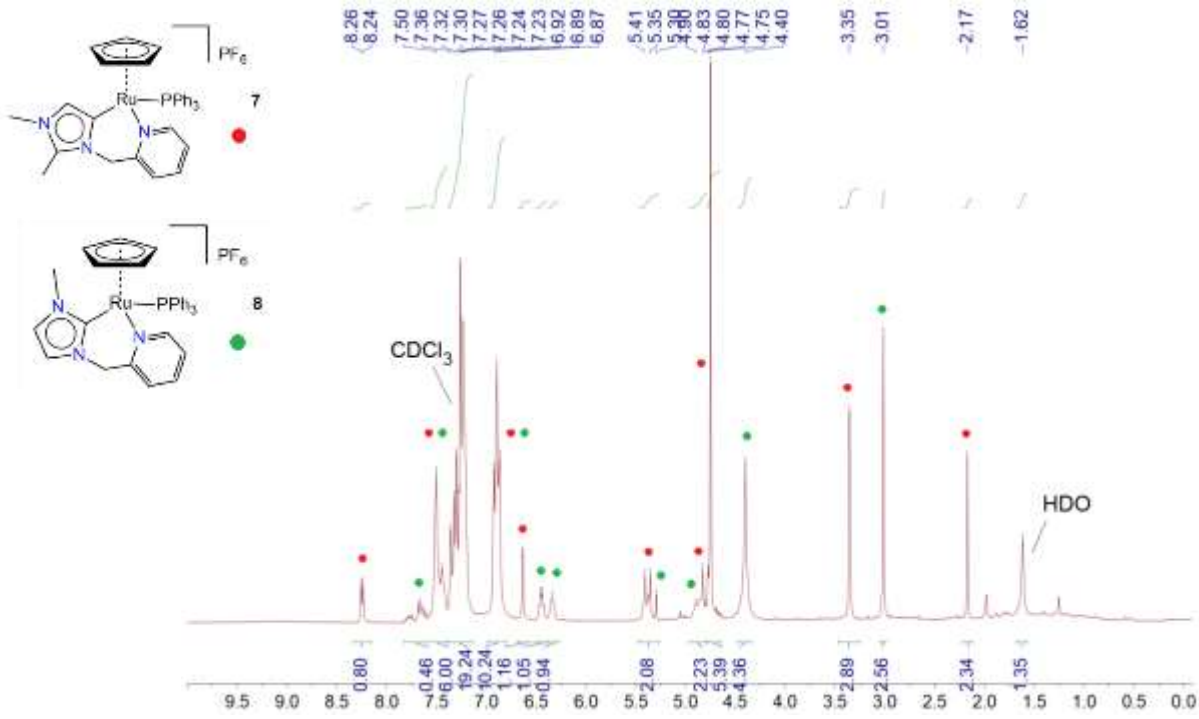

Figure S26. ^{1}H NMR spectrum (300 MHz, 298 K, $CDCl_3$) of complexes **7/8**.

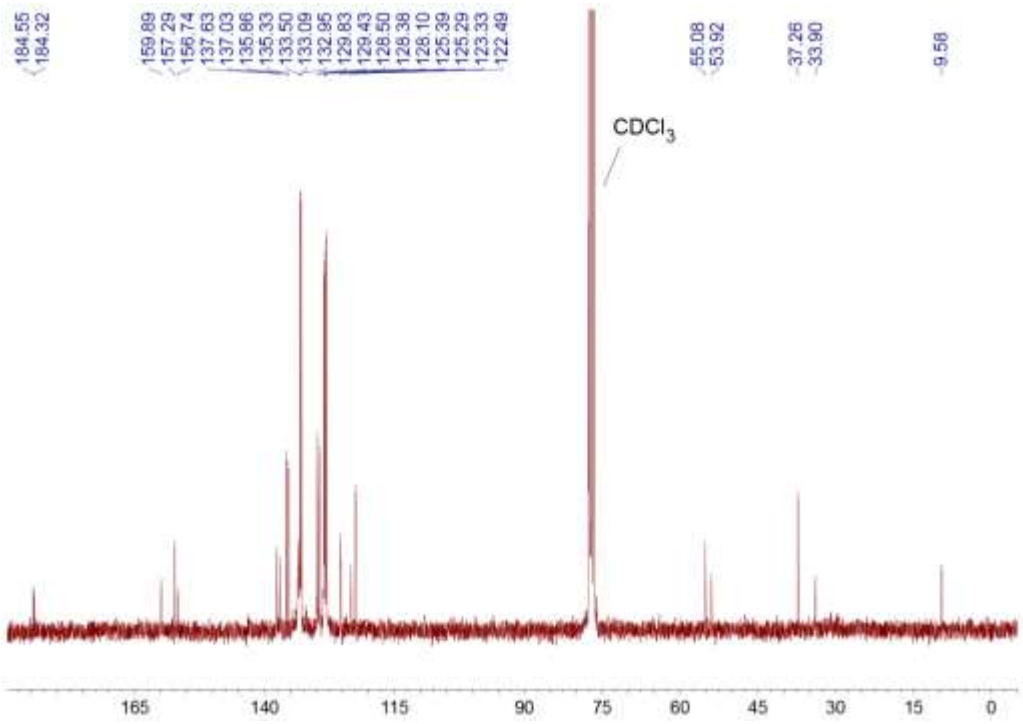

Figure S27. ^{13}C NMR spectrum (76 MHz, 298 K, $CDCl_3$) of complexes **7/8**.

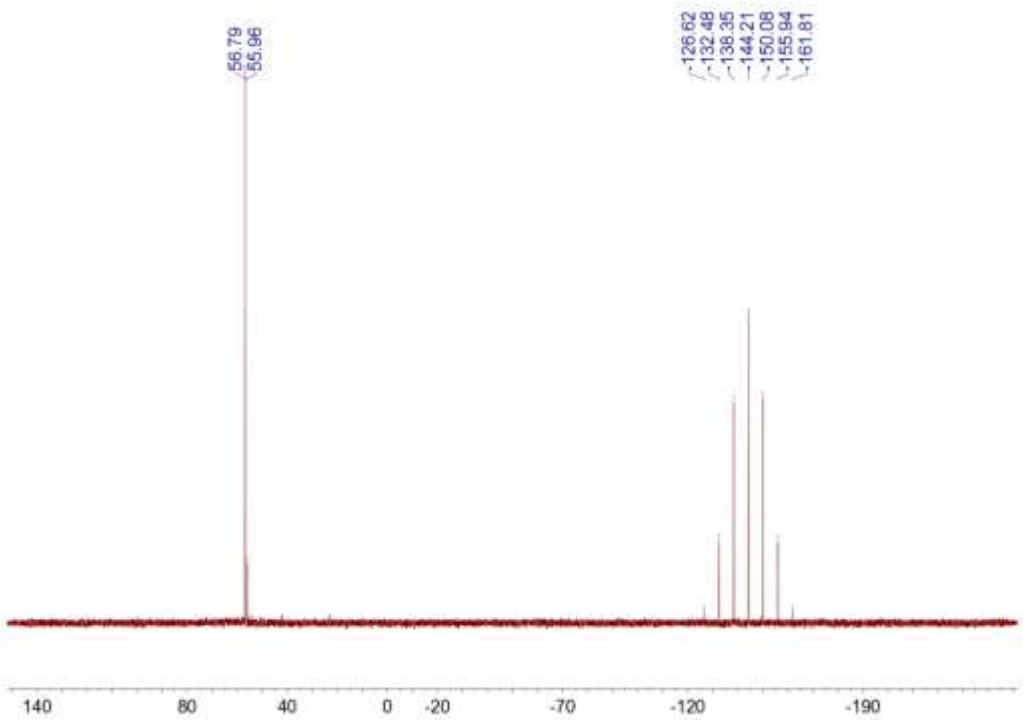

Figure S28. ^{31}P NMR spectrum (122 MHz, 298 K, $CDCl_3$) of complexes **7/8**.

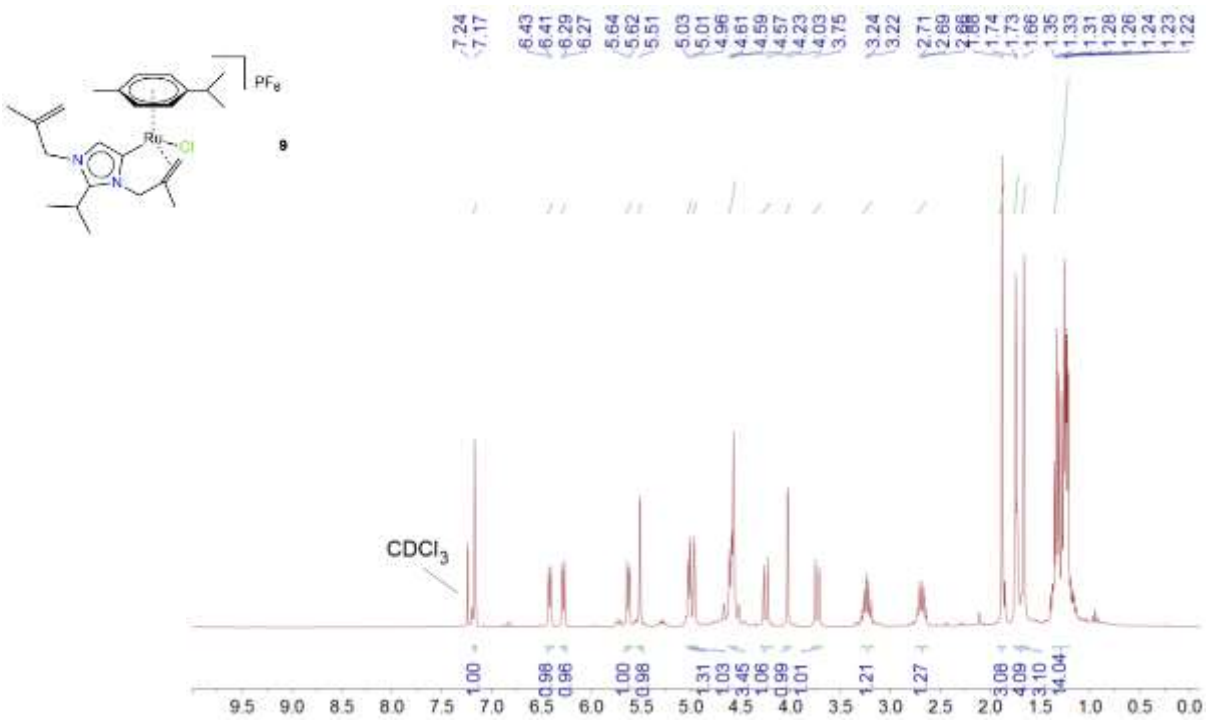

Figure S29. ^{1}H NMR spectrum (300 MHz, 298 K, $CDCl_3$) of complex **9**.

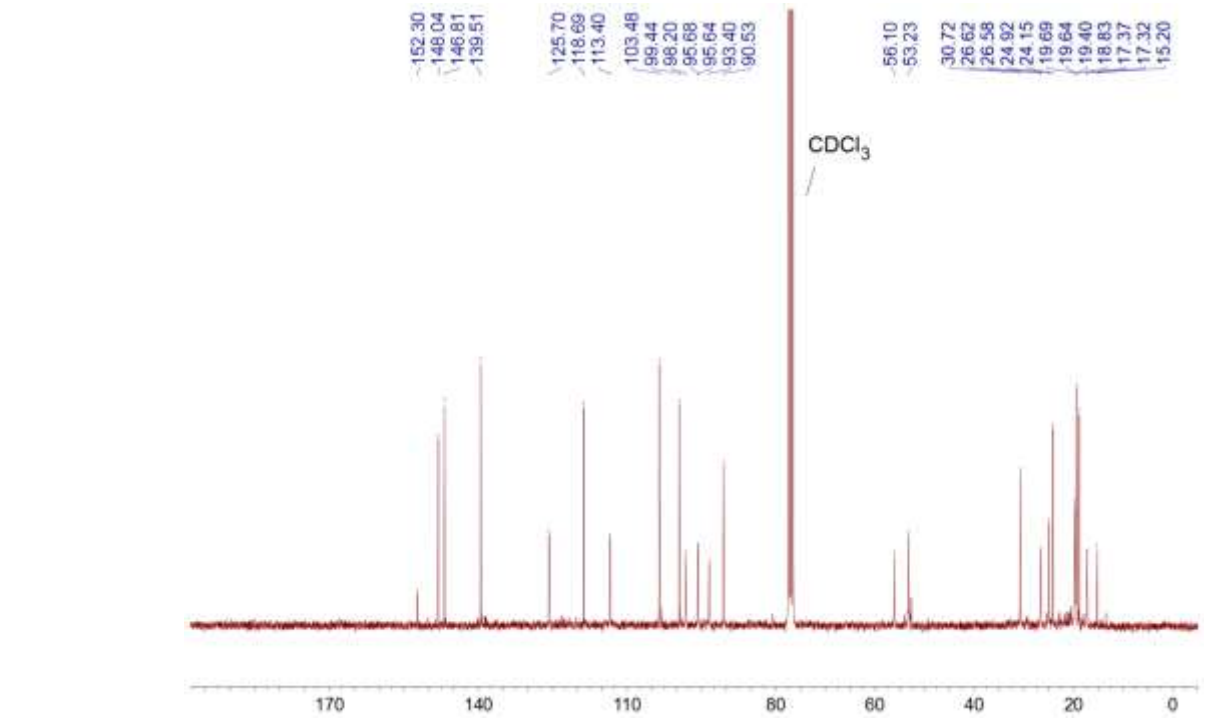

Figure S30. ^{13}C NMR spectrum (76 MHz, 298 K, $CDCl_3$) of complex **9**.

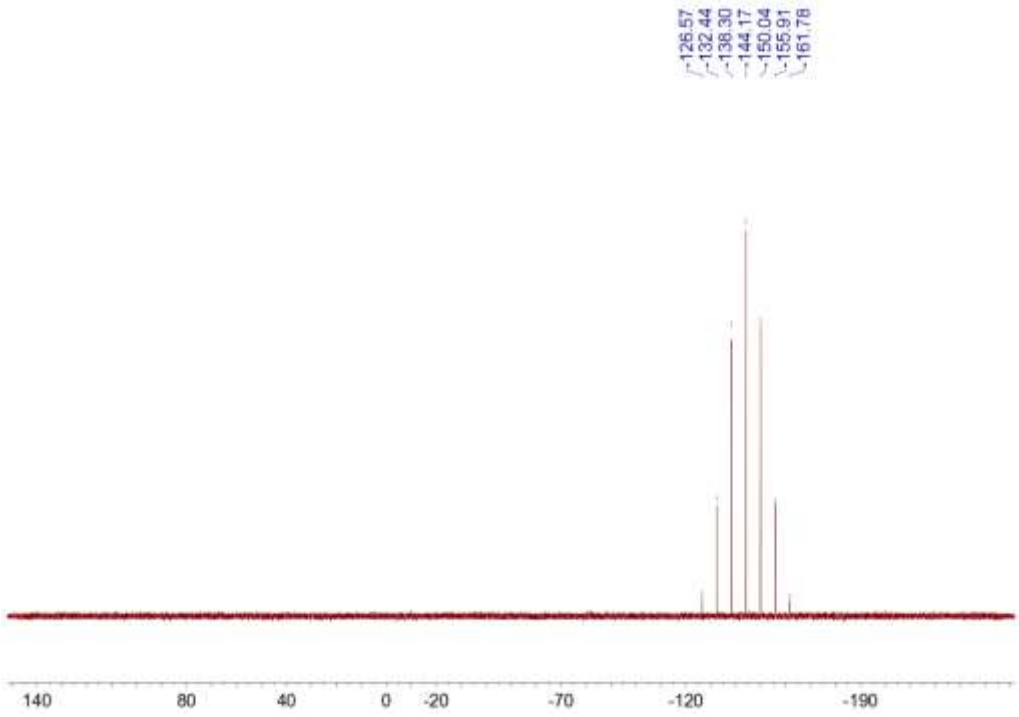

Figure S31. ^{31}P NMR spectrum (122 MHz, 298 K, $CDCl_3$) of complex **9**.

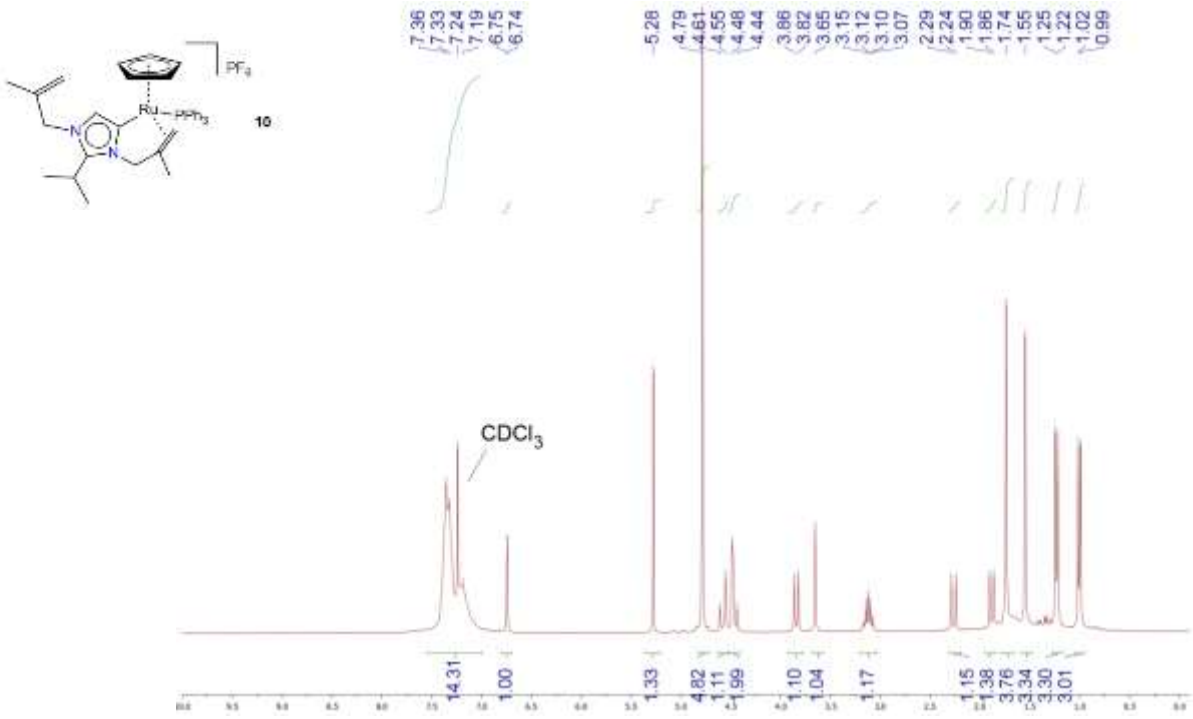

Figure S32. ^{1}H NMR spectrum (300 MHz, 298 K, $CDCl_3$) of complex **10**.

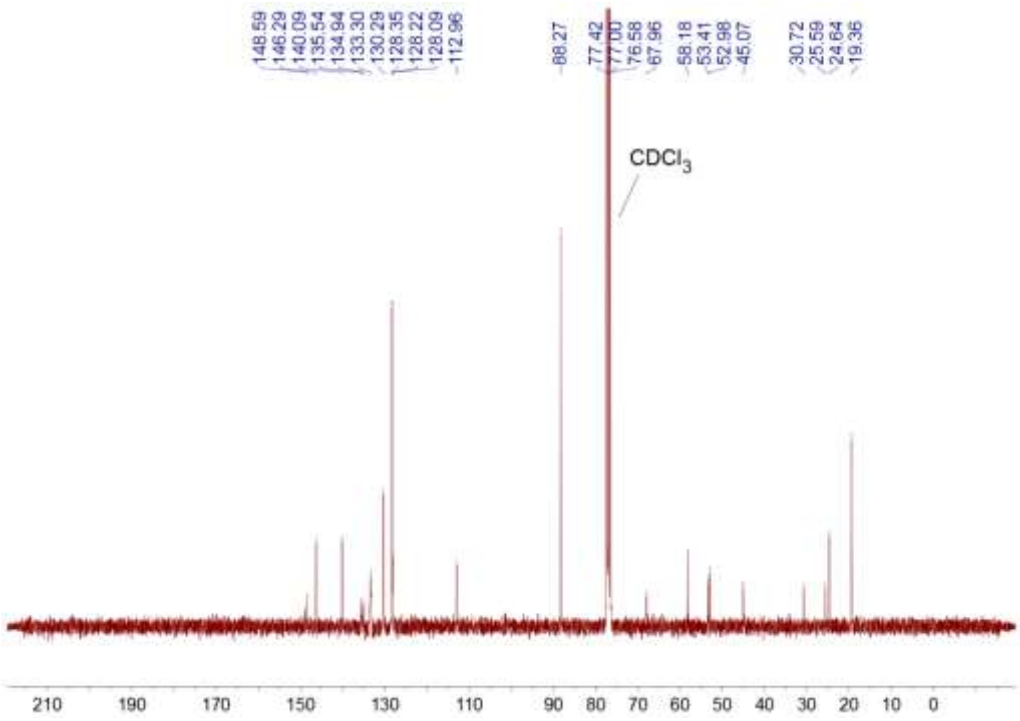

Figure S33. ^{13}C NMR spectrum (76 MHz, 298 K, $CDCl_3$) of complex **10**.

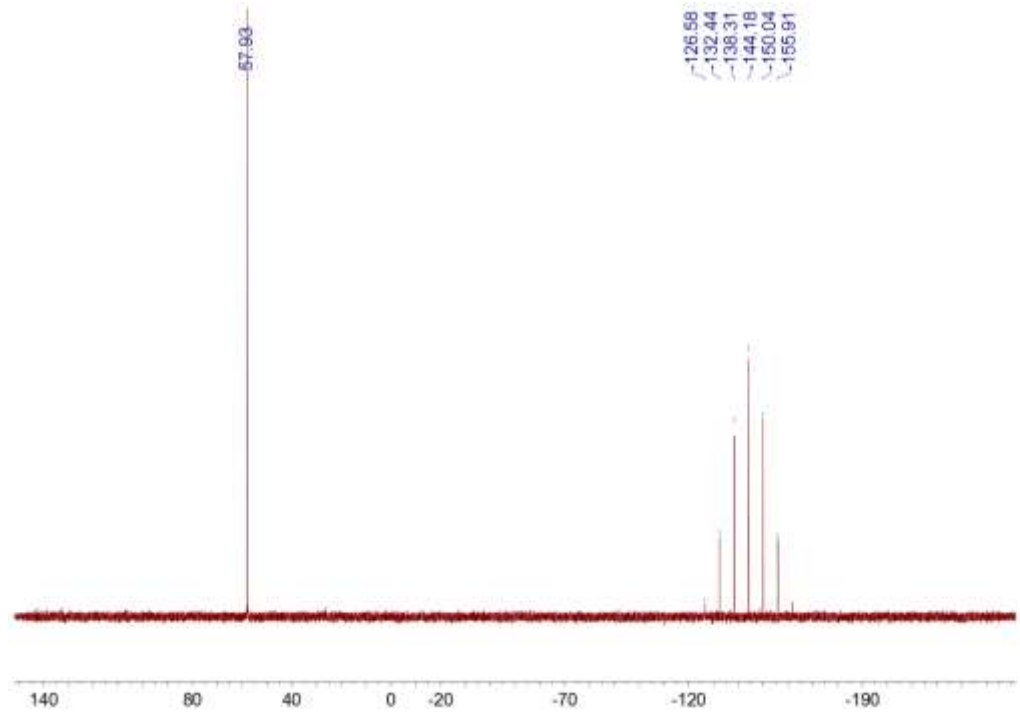

Figure S34. ^{31}P NMR spectrum (122 MHz, 298 K, $CDCl_3$) of complex **10**.

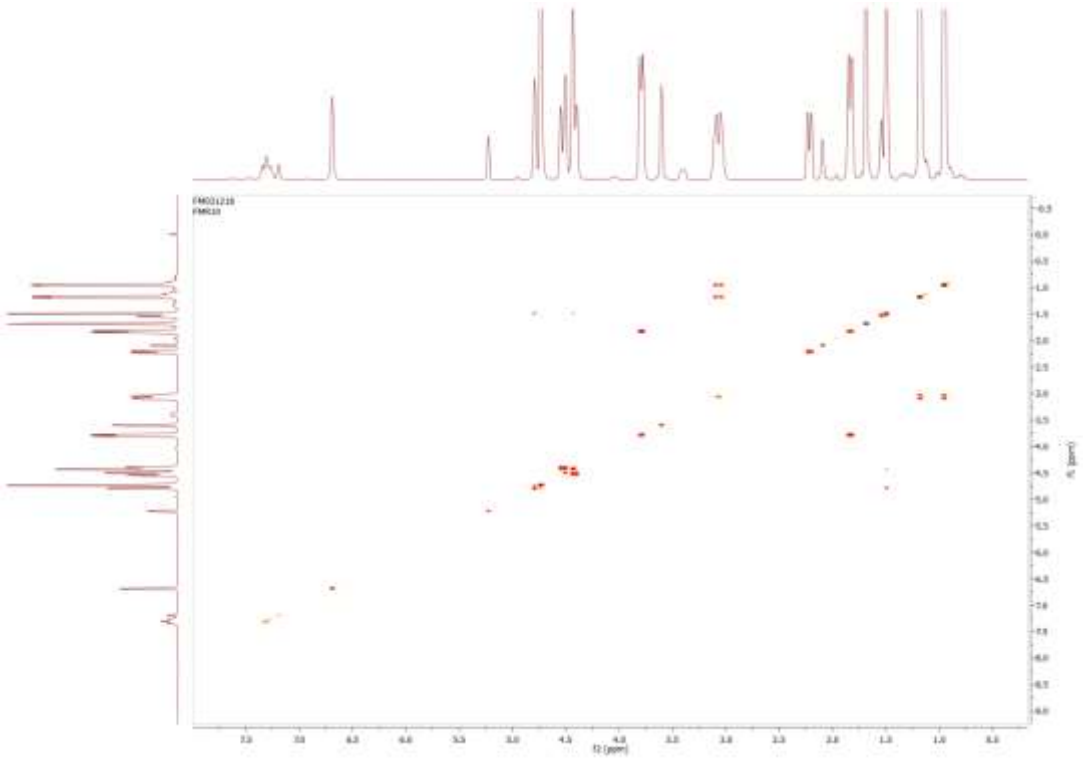

Figure S35. HSQC NMR spectrum (400, 100 MHz, 298 K, $CDCl_3$) of complex **10**.

3. Crystallographic details

Table S1. Crystal data and structure refinement for [H**L1**]Cl, [H**L4**]Cl, **1**, **3**.

	[H**L1]**Cl	**[**H**L4]**Cl	**1**	**3**
CCDC Identifier	1843098	1843100	1843096	1843103
Emp. formula	$C_9H_{15}N_2F_6P$	$C_{14}H_{23}ClN_2$	$C_{19}H_{28}ClF_6N_2PRu$	$C_{128}H_{136}F_{24}N_8P_8Ru_4$
Form. weight (g.mol^{-1})	296.20	254.79	565.92	2894.48
Crystal system	monoclinic	trigonal	monoclinic	monoclinic
Space group	*P2$_1$/c*	*P3$_2$21*	*P2$_1$/c*	*Cc*
Crystal descr.	yellow block	colourless block	yellow prism	gold block
a (Å)	6.5921(4)	7.8674(1)	13.4504(2)	20.1114(1)
b (Å)	13.8855(7)	7.8674(2)	13.8832(3)	19.4730(1)
c (Å)	14.0294(8)	21.086(2)	11.9684(3)	31.887(2)
α (°)	90	90	90	90
β (°)	92.682(3)	90	100.215(2)	100.516(2)
γ (°)	90	120	90	90
Volume (Å^3)	1282.77(1)	1130.3(4)	2199.49(8)	12278.2(2)
Z	4	3	4	4
Abs. coeff. (m.mm^{-1})	0.272	0.237	0.966	0.677
F(000)	608.0	414.0	1144.0	5888.0
Independent refl.	2625	1592	4527	25310
Completeness (%)	99.8	99.6	91.9	99.8
Data/Restr/Para	2625/0/166	1592/0/122	4527/0/277	25310/2/1562
Goodness of fit on F^2	1.064	1.043	1.031	1.049
Final R$_1$ indexes	0.0418	0.0418	0.0325	0.0333
wR$_2$ indices (all data)	0.1065	0.1054	0.0744	0.0730
Largest diffr. peak and hole (e.Å^{-3})	0.33/-0.28	0.20/-0.20	1.11/-0.63	0.59/-0.42

Table S2. Crystal data and structure refinement for **5**, **6**, **7/8.CH$_2$Cl$_2$**, **7/8.CHCl$_3$**.

	5	**6**	**7/8.CH$_2$Cl$_2$**	**7/8.CHCl$_3$**
CCDC Identifier	1843097	1843099	1843101	1843102
Emp. formula	$C_{32}H_{34}F_6N_2P_2Ru$	$C_{24}H_{30}N_3F_6PClRu$	$C_{33.5}H_{20}F_6N_3P_2Ru$	$C_{68}H_{65}Cl_3F_{12}N_6P_4Ru_2$
Form. weight (g.mol^{-1})	723.62	642.00	741.44	1626.63
Crystal system	monoclinic	monoclinic	monoclinic	triclinic
Space group	*P2$_1$/n*	*P2$_1$/c*	*P2$_1$/n*	*P-1*
Crystal descr.	yellow prism	yellow blade	yellow fragment	yellow block
a (Å)	17.8511(6)	8.2722(1)	13.6883(9)	14.8003(7)
b (Å)	9.6153(2)	11.3526(1)	14.8014(9)	15.2415(1)
c (Å)	18.9847(6)	27.375(4)	15.5452(1)	16.7390(1)
α (°)	90	90	90	85.024(2)
β (°)	111.505(4)	91.752(4)	96.467(2)	80.728(2)
γ (°)	90	90	90	77.631(2)
Volume (Å^3)	3031.76(2)	2569.6(6)	3129.5(3)	3634.8(4)
Z	4	4	4	2
Abs. coeff. (m.mm^{-1})	0.686	0.839	0.668	0.688
F(000)	1472.0	1300.0	1480.0	1644.0
Independent refl.	6195	4699	6443	13308
Completeness (%)	90.4	99.7	99.5	99.7
Data/Restr/Para	6195/60/428	4699/3/347	6443/156/479	13308/71/841
Goodness of fit on F^2	1.023	1.049	1.032	1.058
Final R$_1$ indexes	0.0460	0.0245	0.0495	0.0866
wR$_2$ indices (all data)	0.0995	0.0615	0.1153	0.1975
Largest diffr. peak and hole (e.Å^{-3})	0.63/-0.63	0.57/-0.55	1.07/-1.81	4.62/-4.10

Table S3. Crystal data and structure refinement for **10**.

	10
CCDC Identifier	1843104
Emp. formula	$C_{37}H_{42}F_6N_2P_2Ru$
Form. weight (g.mol^{-1})	791.73
Crystal system	orthorhombic
Space group	*Pbca*
Crystal descr.	yellow prism
a (Å)	14.8783(9)
b (Å)	18.7535(2)
c (Å)	25.0075(2)
α (°)	90
β (°)	90
γ (°)	90
Volume (Å^3)	6977.6(7)
Z	8
Abs. coeff. (m.mm^{-1})	0.603
F(000)	3248.0
Independent refl.	7200
Completeness (%)	99.9
Data/Restr/Para	7200/0/474
Goodness of fit on F^2	1.043
Final R_1 indexes	0.0311
wR_2 indices (all data)	0.0661
Largest diffr. peak and hole (e.Å^{-3})	0.35/-0.40

Table S4. Selected bond lengths and angles for [H**L1**]Cl, [H**L4**]Cl, **1**, **3**, **5**, **6**, **7/8.CH$_2$Cl$_2$**, **7/8.CHCl$_3$**, **10**.

Description	[H**L1**]Cl	[H**L4**]Cl	**1**	**3**	**5**	**6**	**7**	**8**	**10**
Ru1-C4	-	-	2.045(3)	2.0586(2)	2.032(4)[c]	2.045(2)	2.057(6)	2.099(4)[c]	2.046(2)
Ru1-Cg[a]	-	-	1.728(3)	1.866(3)	1.905(3)	1.691(2)	1.853(6)	1.856(6)	1.899(4)
Ru-Cl1	-	-	2.4114(7)	-	-	2.4075(6)	-	-	-
Ru-P1	-	-	-	2.2948(2)	2.307(1)	-	2.2863(2)	2.3102(1)	2.3175(6)
Ru1-C4-C5	-	-	138.5(2)	139.1(5)	135.2(3)[c]	135.04(2)	137.3(5)	130.5(4)[c]	109.31(1)
N1-C3-C2	113.6(2)	114.4(3)	105.4(2)	107.6(5)	108.2(3)	-	-	-	106.95(2)
N3-C6-C7	-	-	-	-	-	112.97(2)	128.4(7)	121.3(7)	-
C4-Ru1-Ca[b]	-	-	89.49(1)	90.45(2)	89.10(1)[c]	-	-	-	91.31(8)
C4-Ru1-N3	-	-	-	-	-	85.94(8)	86.6(2)	85.7(3)[c]	-
Cl1-Ru1-C4	-	-	83.69(8)	-	-	87.17(6)	-	-	-
P1-Ru1-C4	-	-	-	85.01(2)	86.71(1)[c]	-	89.72(2)	89.1(2)[c]	87.62(6)
C1-C2-C3-N1	10.2(3)	4.3(5)	- 122.675(2)	- 112.194(4)	- 108.369(4)	-	-	-	- 116.977(2)
N3-C7-C6-N1	-	-	-	-	-	-48.60(3)	- 55.077(6)	- 51.739(4)	-

[a] Cg = centroid of arene/cyclopentadienyl moiety. [b] Ca = Average position between two carbon atoms belonging to the alkene moiety. [c] C2 replaces C4 for C(2)-bound (normal) NHC.

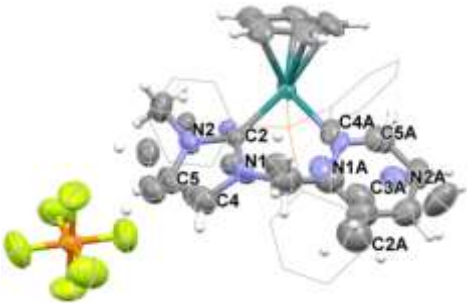

Figure S36: Perspective view of **7** and **8** when CH_2Cl_2 is used as crystallizing solvent.

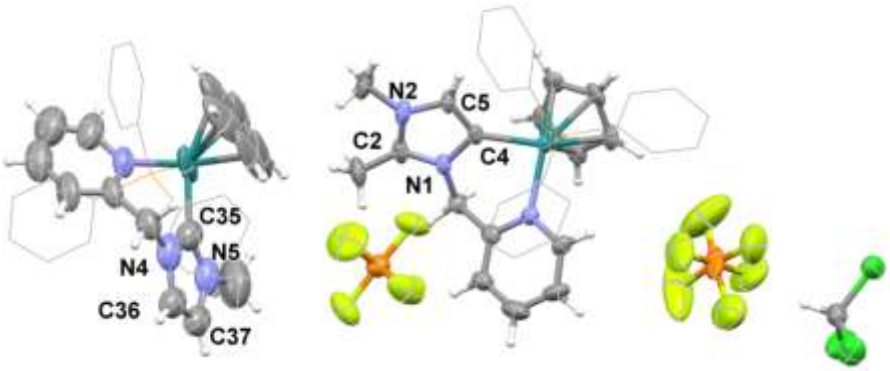

Figure S37: Perspective view of **7** and **8** when $CHCl_3$ is used as crystallizing solvent.

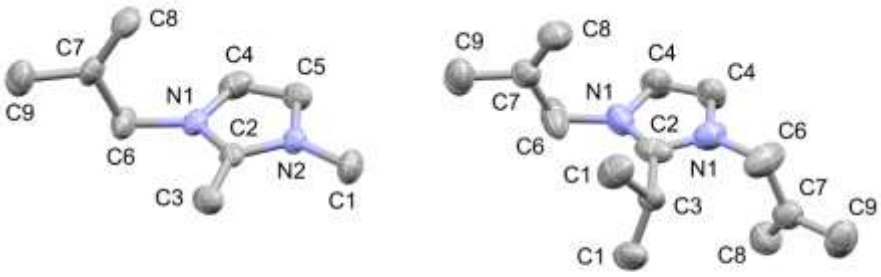

[HL**1**]Cl [HL**4**]Cl

Figure S38: ORTEP plots of compounds [H**L1**]Cl and [H**L4**]Cl. Thermal ellipsoids are drawn at 50% level. For clarity, non-coordinating anions and hydrogens are omitted.

4. Acidity measurements

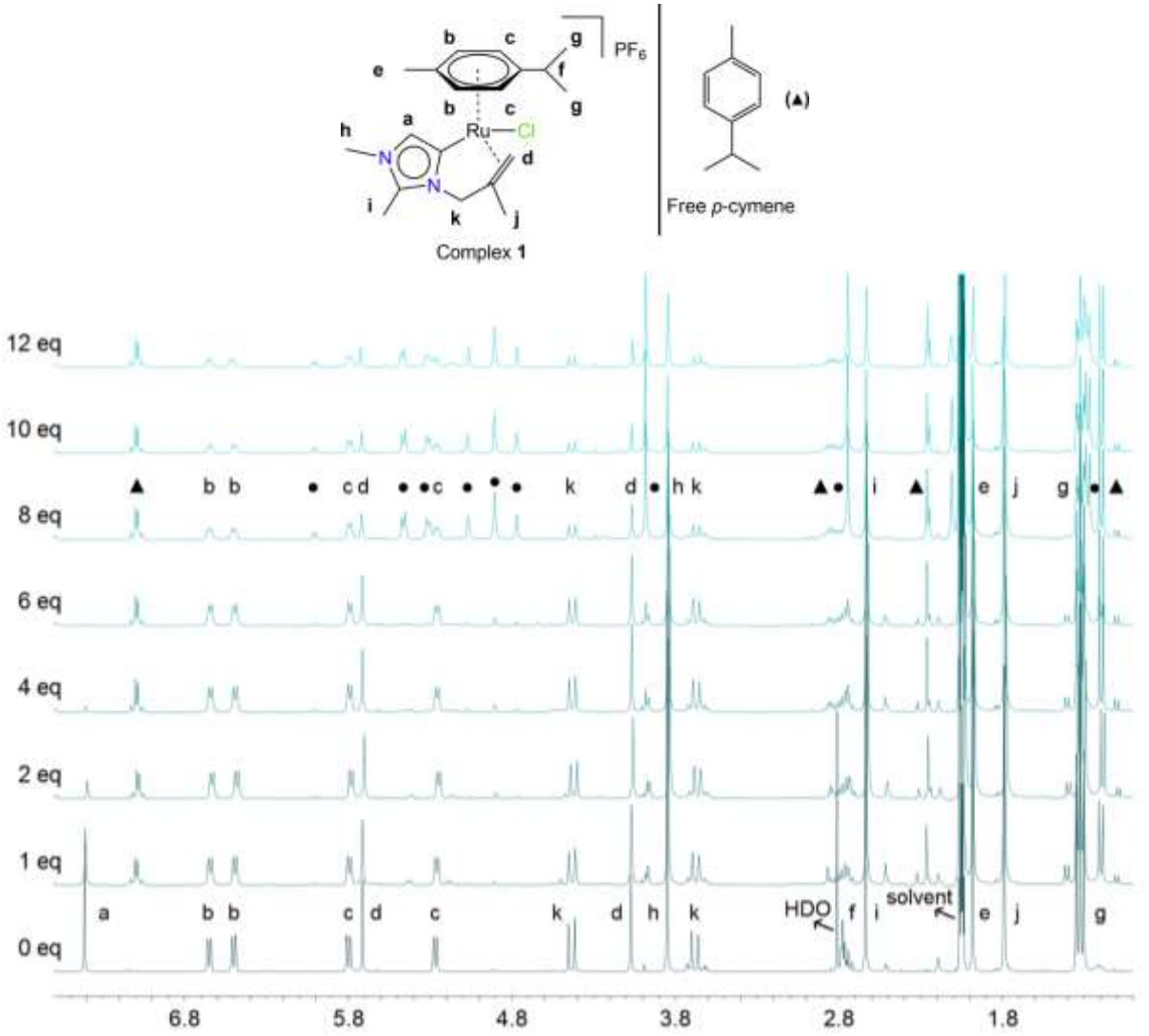

Figure S39: ^{1}H NMR spectra (300 MHz, 298 K, $(CD_3)_2CO$, δ_H 1.0–7.6) of complex **1** with stoichiometric addition of DCl. Signals **a**-**j** correspond to those of complex **1**. The signals ▲ and ● correspond to those of free *p*-cymene and [Ru-aNHC] complex bearing a free *N*-alkenyl substituent, respectively.

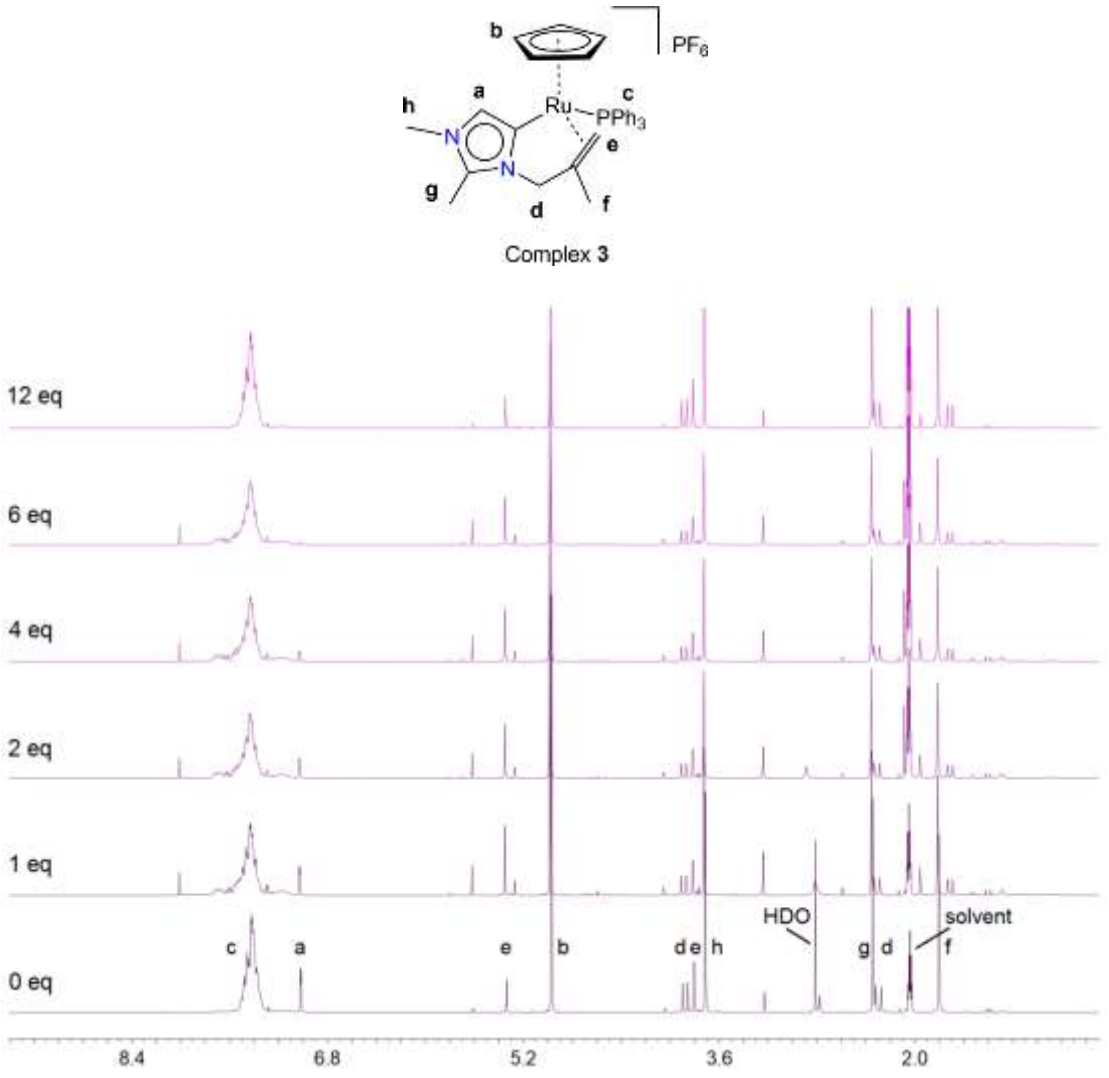

Figure S40: ^{1}H NMR spectra (300 MHz, 298 K, $(CD_3)_2CO$, δ_H 0.5–9.4) of complex **3** with stoichiometric addition of DCl. Signals (a)-(g) correspond to the different moieties indicated of complex **3**. Solvent = acetone-d_6. The signal observed at δ_H 8.01 does not correspond to the free imidazolium salt [H**L1**]Cl (see ^{1}H NMR spectrum on p. 2).

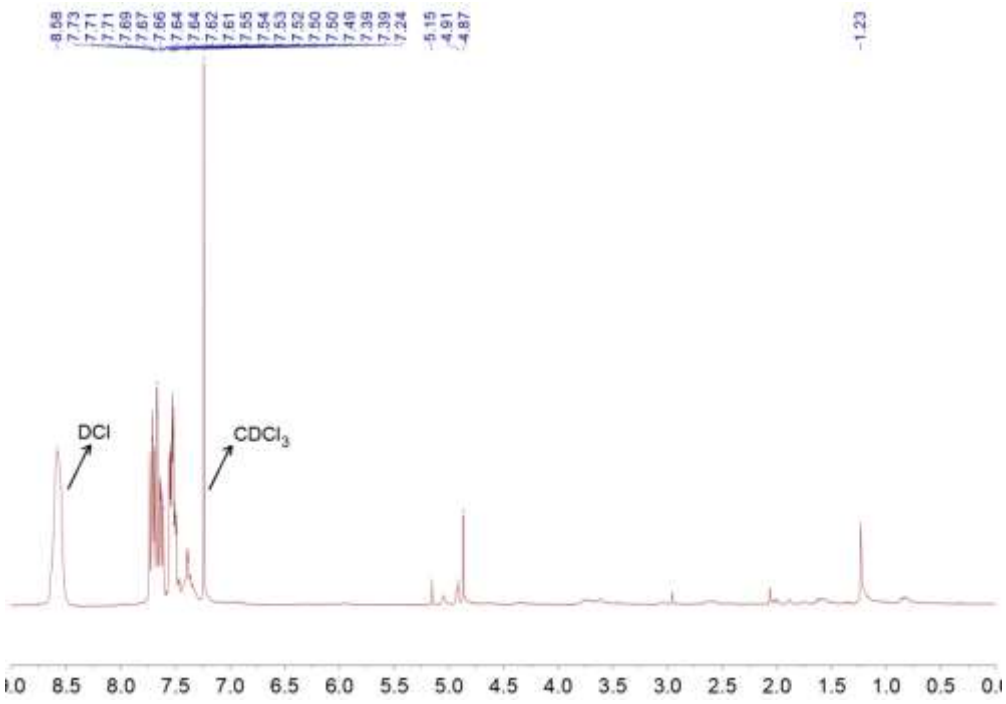

Figure S41: ^{1}H NMR spectrum (300 MHz, 298 K, $CDCl_3$) of complex **3** after addition of 12 eq. DCl over a period of two weeks.

5. Catalytic details

Table S5: Transfer hydrogenation of benzophenone using complexes **1** or **3**; optimization of conditions.[a]

Entry	Complex	Temp (°C)	Base	Conversion[b] (%)	
				2h	6h
1	[(*p*-cym)$RuCl_2$]$_2$	110	KO^{t}Bu	-	8[c]
2	[CpRuCl(PPh_3)$_2$]	110	KO^{t}Bu	-	6[c]
3	-	110	KOH	1	2[c]
4	-	110	KO^{t}Bu	3	6[c]
5	**1**	110	-	5	28
6	**3**	110	-	2	5
7	**1** (3 mol%)	110	KOH	72	95
8	**1**	110	KO^{t}Bu	69	94
9	**3**	110	KO^{t}Bu	32	69
10	**3**	110	KOH	17	42
11	**1** (0.5 mol%)	110	KOH	9	37
12	**1**	110	KOH (10 mol%)	64	92
13	**1**	25	KOH	4	10

[a] General conditions: Benzophenone (0.6 mmol), ^{i}PrOH (5 mL), base (5 mol%), [Ru] (1 mol%), 110 °C. Base used depending on Ru catalyst: KOH (**1**); KO^{t}Bu (**3**). [a] Mixture of complexes as isolated after purification. [b] Determined by GC, based on the average of at least two runs. Yields in parentheses are based on ^{1}H NMR spectroscopy. [c] After 18 hours' reaction time.

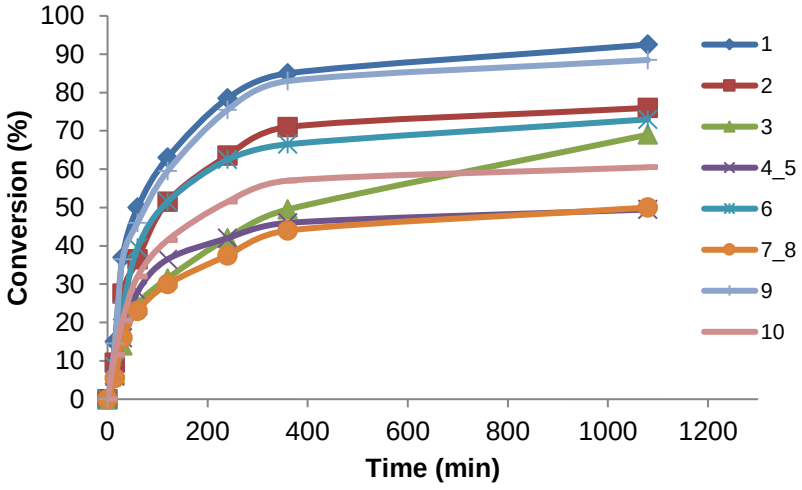

Figure S42: Time-resolved conversion profiles in the transfer hydrogenation reactions of **1-10**. General conditions: benzophenone (0.6 mmol), ^{i}PrOH (5 mL), base (5 mol%), [Ru] (1 mol%), 110 °C. Base used depending on Ru catalyst: KOH (**1**, **2**, **6**, **9**); KO^{t}Bu (**3-5**, **7**, **8**, **10**).

Complexes **4/5** and **7/8** were used as a ~50/50 mixture of complexes as isolated after purification. Conversions determined by GC, based on the average of at least two runs.

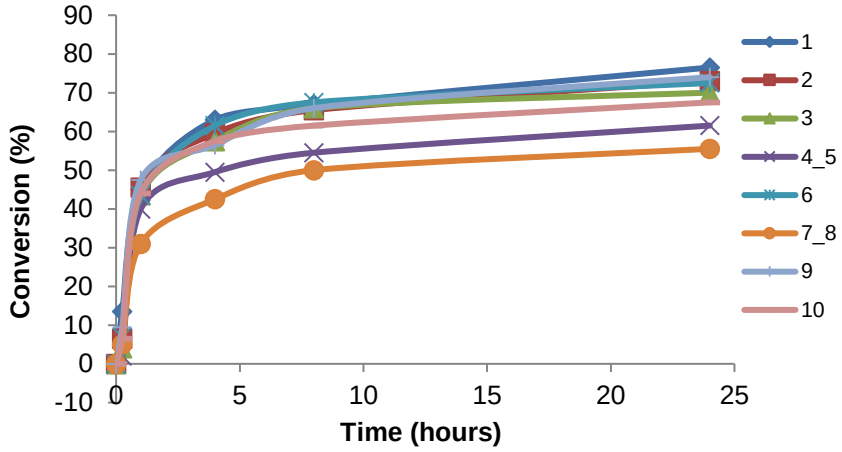

Figure S43: Time-resolved conversion profiles in the alcohol oxidation reactions of **1-10**. General conditions: ±1-phenylethanol (1 mmol), o-dichlorobenzene (5 mL), KO^{t}Bu (5 mol%), [Ru] (5 mol%), hexamethylbenzene (0.1 mmol), 150 °C. Complexes **4/5** and **7/8** were used as a ~50/50 mixture of complexes as isolated after purification. Conversions determined by GC, based on the average of at least two runs.

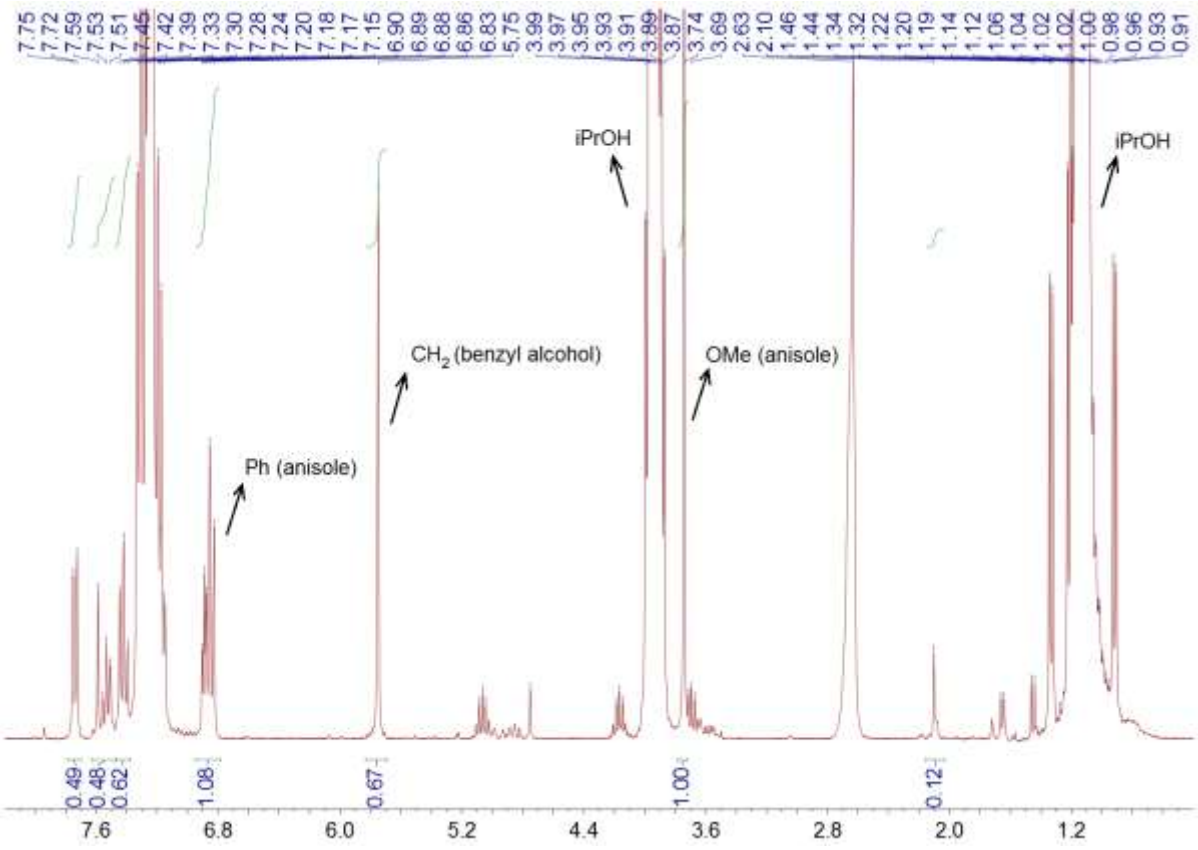

Figure S44: ^{1}H NMR spectrum (300 MHz, 298 K, $CDCl_3$) spectrum of transfer hydrogenation reaction mixture using complex **1**. General conditions: Benzophenone (0.6 mmol), ^{i}PrOH (5

mL), KOH (5 mol%), [**1**] (1 mol%), 110 °C. Aliquot taken after 2 h reaction time. Internal standard: anisole.

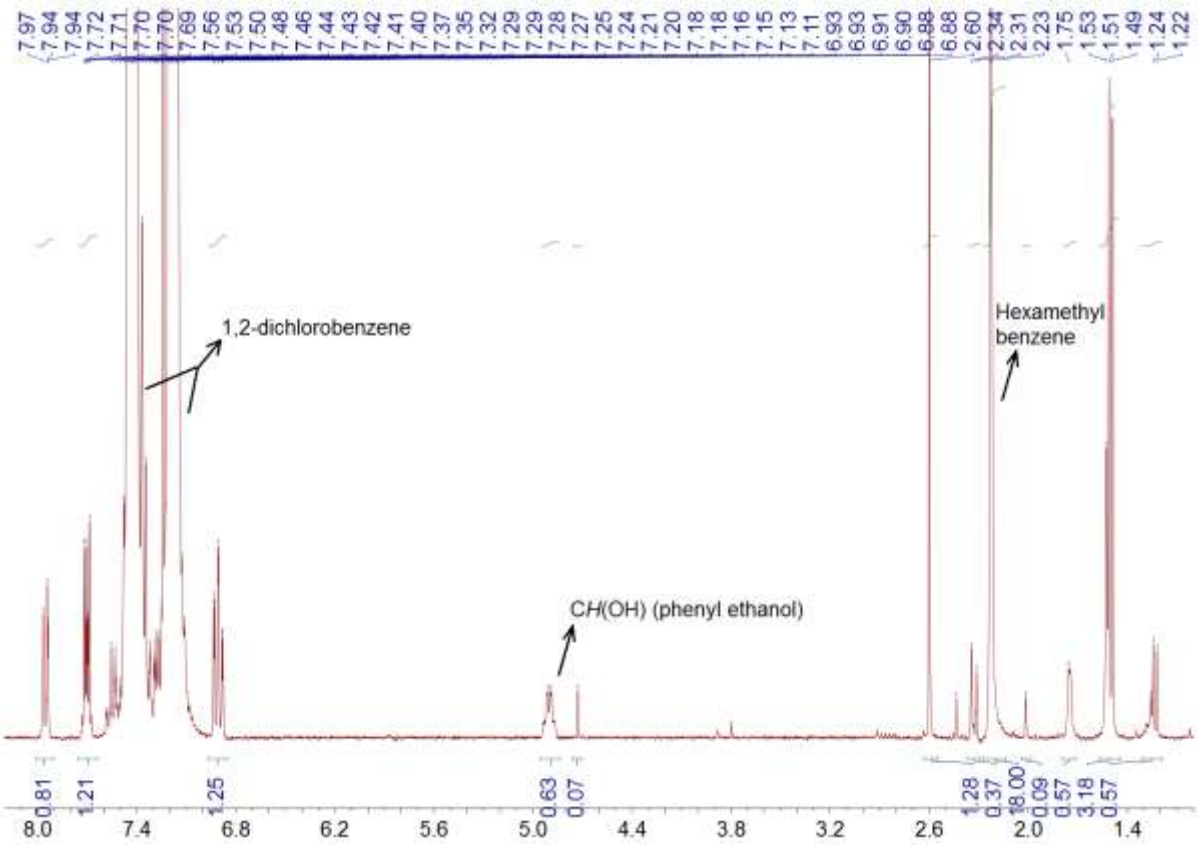

Figure S45: ^{1}H NMR spectrum (300 MHz, 298 K, $CDCl_3$) of alcohol oxidation reaction mixture using complex **1**. General conditions: ±1-Phenylethanol (1 mmol), *o*-dichlorobenzene (5 mL), KO^{t}Bu (5 mol%), [**1**] (5 mol%), hexamethylbenzene (1 mmol), 150 °C. Aliquot taken after 4 h reaction time.